Unifying the known and unknown microbial coding sequence space

Chiara Vanni[1,2], Matthew S. Schechter[1,3], Silvia G. Acinas[4], Albert Barberán[5], Pier Luigi Buttigieg[6], Emilio O. Casamayor[7], Tom O. Delmont[8], Carlos M. Duarte[9], A. Murat Eren[3,10], Robert D. Finn[11], Renzo Kottmann[1], Alex Mitchell[11], Pablo Sanchez[4], Kimmo Siren[12], Martin Steinegger[13,14], Frank Oliver Glöckner[15,16,2], Antonio Fernandez-Guerra[1,17 *]

Affiliations

1 Microbial Genomics and Bioinformatics Research Group, Max Planck Institute for Marine Microbiology, Celsiusstraße 1, 28359, Bremen, Germany

2 Jacobs University Bremen, Campus Ring 1, 28759 Bremen, Germany

3 Department of Medicine, University of Chicago, Chicago, IL 60637, USA

4 Department of Marine Biology and Oceanography, Institut de Ciènces del Mar, CSIC, Barcelona, Spain.

5 Department of Environmental Science, University of Arizona, Tucson, 85721 AZ, USA

6 Alfred Wegener Institute, Helmholtz Centre for Polar and Marine Research, Am Handelshafen 12, 27570 Bremerhaven, Germany

7 Center for Advanced Studies of Blanes CEAB-CSIC, Spanish Council for Research, Blanes, Spain

8 Génomique Métabolique, Genoscope, Institut François Jacob, CEA, CNRS, Univ Evry, Université Paris-Saclay, 91057 Evry, France

9 Red Sea Research Centre (RSRC) and Computational Bioscience Research Center (CBRC), King Abdullah University of Science and Technology, Thuwal 23955, Saudi Arabia

10 Josephine Bay Paul Center, Marine Biological Laboratory, Woods Hole, MA 02543, USA

11 European Molecular Biology Laboratory, European Bioinformatics Institute (EMBL-EBI), Wellcome Genome Campus, Hinxton, Cambridge CB10 1SD, UK

12 Section for Evolutionary Genomics, The GLOBE Institute, University of Copenhagen, Copenhagen, Denmark

13 School of Biological Sciences, Seoul National University, Seoul, 08826, South Korea

14 Institute of Molecular Biology and Genetics, Seoul National University, Seoul, 08826, South Korea

15 University of Bremen, MARUM, Leobener Str. 8, 28359 Bremen, Germany
Life Sciences and Chemistry, Campus Ring 1, 28759 Bremen, Germany

16 Computing Center, Helmholtz Center for Polar and Marine Research, Am Handelshafen 12, 27570 Bremerhaven, Germany

17 Lundbeck GeoGenetics Centre, The Globe Institute, University of Copenhagen, 1350 Copenhagen, Denmark

*Corresponding author: Antonio Fernandez-Guerra, antonio.fernandez-guerra@sund.ku.dk

Abstract

Genes of unknown function are among the biggest challenges in molecular biology, especially in microbial systems, where 40%-60% of the predicted genes are unknown. Despite previous attempts, systematic approaches to include the unknown fraction into analytical workflows are still lacking. Here, we propose a conceptual framework and a computational workflow that bridge the known-unknown gap in genomes and metagenomes. We showcase our approach by exploring 415,971,742 genes predicted from 1,749 metagenomes and 28,941 bacterial and archaeal genomes. We quantify the extent of the unknown fraction, its diversity, and its relevance across multiple biomes. Furthermore, we provide a collection of 283,874 lineage-specific genes of unknown function for *Cand*. Patescibacteria, being a significant resource to expand our understanding of their unusual biology. Finally, by identifying a target gene of unknown function for antibiotic resistance, we demonstrate how we can enable the generation of hypotheses that can be used to augment experimental data.

Introduction

Thousands of isolate, single-cell, and metagenome-assembled genomes are guiding us towards a better understanding of life on Earth (Almeida et al., 2019; Cross et al., 2019; Delmont et al., 2020; Hug et al., 2016; Kopf et al., 2015; Pachiadaki et al., 2019; Pasolli et al., 2019; Sunagawa et al., 2015). At the same time, the ever-increasing number of genomes and metagenomes, unlocking uncharted regions of life's diversity, (Brown et al., 2015; Eloe-Fadrosh et al., 2016; Hug et al., 2016) are providing new perspectives on the evolution of life (Parks et al., 2018; Spang et al., 2015). However, our rapidly growing inventories of new genes have a glaring issue: between 40% and 60% cannot be assigned to a known function (Almeida et al., 2020; Bernard, Pathmanathan, Lannes, Lopez, & Bapteste, 2018; Carradec et al., 2018; Price et al., 2018). Current analytical approaches for genomic and metagenomic data (Chen et al., 2019; Franzosa et al., 2018; Huerta-Cepas et al., 2017; Mitchell et al., 2020; Quince, Walker, Simpson, Loman, & Segata, 2017) generally do not include this uncharacterized fraction in downstream analyses, constraining their results to conserved pathways and housekeeping functions (Quince et al., 2017). This inability to handle the unknown is an immense impediment to realizing the potential for discovery of microbiology and molecular biology at large (Bernard et al., 2018; Hanson, Pribat, Waller, & Crécy-Lagard, 2010). Predicting function from traditional single sequence similarity appears to have yielded all it can (Arnold, 1998, 2018; Brandenberg, Fasan, & Arnold, 2017), thus several groups have attempted to resolve gene function by other means. Such efforts include combining biochemistry and crystallography (Jaroszewski et al., 2009); using environmental co-occurrence (Buttigieg et al., 2013); by grouping those genes into evolutionarily related families (Bateman, Coggill, & Finn, 2010; Brum et al., 2016; Wyman, Avila-Herrera, Nayfach, & Pollard, 2018; Yooseph et al., 2007); using remote homologies (Bitard-Feildel & Callebaut, 2017; Lobb, Kurtz, Moreno-Hagelsieb, & Doxey, 2015); or more recently using deep learning approaches (Bileschi et al., 2019; Liu, 2017). In 2018, Price et al. (Price et

80 al., 2018) developed a high-throughput experimental pipeline that provides mutant phenotypes
81 for thousands of bacterial genes of unknown function being one of the most promising methods
82 to tackle the unknown. Despite their promise, experimental methods are labor-intensive and
83 require novel computational methods that could bridge the existing gap between the known and
84 unknown coding sequence space (CDS-space).
85 Here we present a conceptual framework and a computational workflow that closes the gap
86 between the known and unknown CDS-space by connecting genomic and metagenomic gene
87 clusters. Our approach adds context to vast amounts of unknown biology, providing an
88 invaluable resource to understand the unknown functional fraction better and boost the current
89 methods for its experimental characterization. The application of our approach to 415,971,742
90 genes predicted from 1,749 metagenomes and 28,941 bacterial and archaeal genomes
91 revealed that the unknown fraction (1) is smaller than expected, (2) is exceptionally diverse, and
92 (3) is phylogenetically more conserved and predominantly lineage-specific at the Species level.
93 Finally, we show how we can connect all the outputs produced by our approach to augment the
94 results from experimental data and add context to genes of unknown function through
95 hypothesis-driven molecular investigations.

Results

A conceptual framework and a computational workflow to unify the known and the unknown coding sequence space

We created the conceptual and technical foundations to unify the known and unknown CDS-space facilitating the integration of the genes of unknown function into ecological, evolutionary and biotechnological investigations. First, we conceptually partitioned the known and unknown fractions into (1) Known with Pfam annotations (K), (2) Known without Pfam annotations (KWP), (3) Genomic unknown (GU), and (4) Environmental unknown (EU) (Fig. 1A). The framework introduces a subtle change of paradigm compared to traditional approaches where our objective is to provide the best representation of the unknown space. We gear all our efforts towards finding sequences without any evidence of known homologies by pushing the search space beyond the *twilight zone* of sequence similarity (Rost, 1999). With this objective in mind, we use gene clusters (GCs) instead of genes as the fundamental unit to compartmentalize the CDS-space owing to their unique characteristics (Fig. 1B). (1) GCs produce a structured CDS-space reducing its complexity (Fig. 1B), (2) are independent of the known and unknown fraction, (3) are conserved across environments and organisms, and (4) can be used to aggregate information from different sources (Fig. 1A). Moreover, the GCs provide a good compromise in terms of resolution for analytical purposes, and owing to their unique properties, one can perform analyses at different scales. For fine-grained analyses, we can exploit the gene associations within each GC; and for coarse-grained analyses, we can create groups of GCs based on their shared homologies (Fig. 1B).

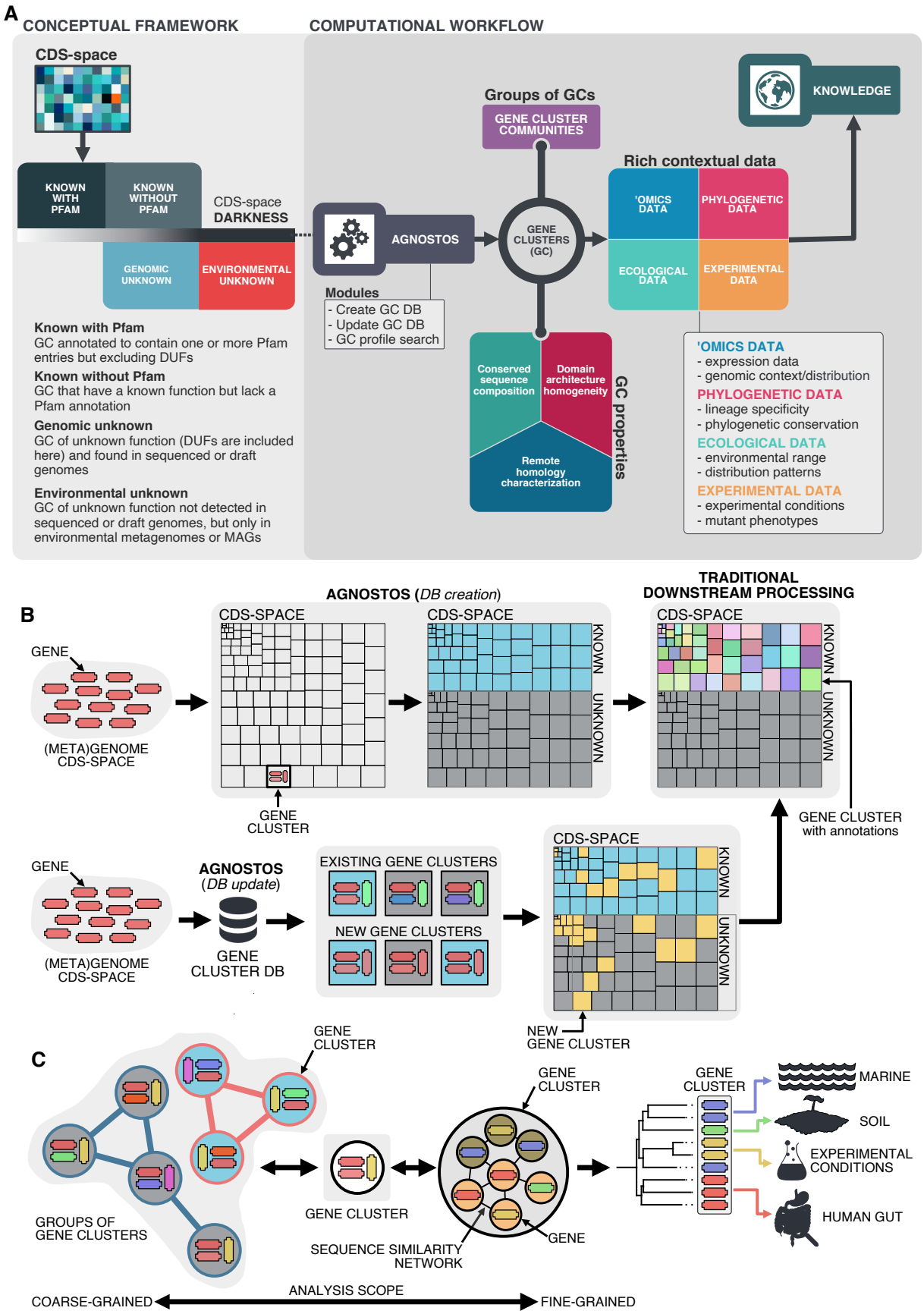
A
CONCEPTUAL FRAMEWORK
COMPUTATIONAL WORKFLOW
CDS-space
KNOWN WITH PFAM
KNOWN WITHOUT PFAM
CDS-space DARKNESS
GENOMIC UNKNOWN
ENVIRONMENTAL UNKNOWN
Known with Pfam
GC annotated to contain one or more Pfam entries but excluding DUFs
Known without Pfam
GC that have a known function but lack a Pfam annotation
Genomic unknown
GC of unknown function (DUFs are included here) and found in sequenced or draft genomes
Environmental unknown
GC of unknown function not detected in sequenced or draft genomes, but only in environmental metagenomes or MAGs
AGNOSTOS
Modules
- Create GC DB
- Update GC DB
- GC profile search
Groups of GCs
GENE CLUSTER COMMUNITIES
GENE CLUSTERS (GC)
Conserved sequence composition
Domain architecture homogeneity
Remote homology characterization
GC properties
Rich contextual data
'OMICS DATA
PHYLOGENETIC DATA
ECOLOGICAL DATA
EXPERIMENTAL DATA
KNOWLEDGE
'OMICS DATA
- expression data
- genomic context/distribution
PHYLOGENETIC DATA
- lineage specificity
- phylogenetic conservation
ECOLOGICAL DATA
- environmental range
- distribution patterns
EXPERIMENTAL DATA
- experimental conditions
- mutant phenotypes
B
AGNOSTOS (DB creation)
TRADITIONAL DOWNSTREAM PROCESSING
GENE
(META)GENOME CDS-SPACE
CDS-SPACE
KNOWN
UNKNOWN
GENE CLUSTER
GENE CLUSTER with annotations
AGNOSTOS (DB update)
GENE CLUSTER DB
EXISTING GENE CLUSTERS
NEW GENE CLUSTERS
NEW GENE CLUSTER
C
GENE CLUSTER
GROUPS OF GENE CLUSTERS
SEQUENCE SIMILARITY NETWORK
GENE
MARINE
SOIL
EXPERIMENTAL CONDITIONS
HUMAN GUT
COARSE-GRAINED
ANALYSIS SCOPE
FINE-GRAINED

118

Figure 1: Conceptual framework to unify the known and unknown CDS-space and integration of the framework in the current analytical workflows (A) Link between the conceptual framework and the computational workflow to partition the CDS-space in the four conceptual categories. AGNOSTOS infers, validates and refines the GCs and combines them in gene cluster communities (GCCs). Then, it classifies them in one of the four conceptual categories based on their level of 'darkness'. Finally, we add context to each GC based on several sources of information, providing a robust framework for generating hypotheses that can be used to augment experimental data. (B) The computational workflow provides two mechanisms to structure the CDS-space using GCs, de novo creation of the GCs (*DB creation*), or integrating the dataset in an existing GC database (*DB update*). The structured CDS-space can then be plugged into traditional analytical workflows to annotate the genes within each GC of the known fraction. With AGNOSTOS, we provide the opportunity to integrate the unknown fraction into the current microbiome analyses easily. C) The versatility of the GCs enables analyses at different scales depending on the scope of our experiments. We can group GCs in gene cluster communities based on their shared homologies to perform coarse-grained analyses. On the other hand, we can design fine-grained analyses using the relationships between the genes in a GC, i.e., detecting network modules in the GC inner sequence similarity network. Additionally, given that GCs are conserved across environments, organisms and experimental conditions give us access to an unprecedented amount of information to design and interpret experimental data.

Driven by the concepts defined in the conceptual framework, we developed AGNOSTOS, a computational workflow that infers, validates, refines, and classifies GCs in the four proposed categories (Fig. 1A; Fig. 1B; Supp. Fig 1). AGNOSTOS provides two operational modules (*DB creation* and *DB update*) to produce GCs with a highly conserved intra-homogeneous structure (Fig. 1B), both in terms of sequence similarity and domain architecture homogeneity; it exhausts any existing homology to known genes and provides a proper delimitation of the unknown CDS-space before classifying each GC in one of the four categories (Methods). In the last step, we decorate each GC with a rich collection of contextual data compiled from different sources or generated by analyzing the GC contents in different contexts (Fig. 1A). For each GC, we also offer several products that can be used for analytical purposes like improved representative sequences, consensus sequences, sequence profiles for MMseqs2 (Steinegger & Soding, 2017) and HHblits (Steinegger, Meier, et al., 2019), or the GC members as a sequence similarity network (Methods). To complement the collection, we also provide a subset of what we define as *high-quality* GCs. The defining criteria are (1) the representative is a complete gene and (2) more than one-third of genes within a GC are complete genes.

Partitioning and contextualizing the coding sequence space of genomes and metagenomes

We used our approach to explore the unknown CDS-space of 1,749 microbial metagenomes derived from human and marine environments, and 28,941 genomes from the GTDB_r86 (Supp Fig 2A). The initial gene prediction of AGNOSTOS (Supp Fig 1) produced 322,248,552 genes from the environmental dataset and assigned Pfam annotations to 44% of them. Next, it clustered the predicted genes in 32,465,074 GCs. For the downstream processing, we kept 3,003,897 GCs (83% of the original genes) after filtering out any GC that contained less than ten genes (Skewes-Cox, Sharpton, Pollard, & DeRisi, 2014) removing 9,549,853 clusters and 19,911,324 singletons (Supp Fig 2A; Supp. Note 1). The validation process selected 2,940,257 *good-quality* clusters (Fig. 1B; Supp. Table 1; Supp. Note 2), which resulted in 43% of them being members of the unknown CDS-space after the classification and remote homology refinement steps (Supp Fig 2A, Supp. Note 3). We build the link between the environmental and genomic CDS-space by expanding the final collection of GCs with the genes predicted from GTDB_r86 (Supp Fig 2A). Our environmental GCs already included 72% of the genes from GTDB_r86; 22% of them created 2,400,037 new GCs, and the rest 6% resulted in singleton GCs (Supp Fig 2A; Supp. Note 4; Supp. Note 5). The final dataset includes 5,287,759 GCs (Supp Fig 2A), with both datasets sharing only 922,599 GCs (Supp Fig 2B). The addition of the GTDB_r86 genes increased the proportion of GCs in the unknown CDS-space to 54%. As the final step, the workflow generated a subset of 203,217 *high-quality* GCs (Supp. Table 2; Supp. Fig 3). In these *high-quality* clusters, we identified 12,313 clusters potentially encoding for small proteins (<= 50 amino acids). Most of these GCs are unknown (66%), which agrees with recent findings on novel small proteins from metagenomes (Sberro et al., 2019). The KWP category contains the largest proportion of incomplete genes (Supp. Table 3), disrupting the detection and assignment of Pfam domains. But it also incorporates sequences with an unusual amino

178 acid composition that has homology to proteins with high levels of disorder in the DPD database
179 (Perdigão, Rosa, & O'Donoghue, 2017) and has characteristic functions of intrinsically
180 disordered proteins (Habchi, Tompa, Longhi, & Uversky, 2014) (IDP) like cellular processes and
181 signaling as predicted by eggNOG annotations (Supp. Table 4).
182 As part of the workflow, each GC is complemented with a rich set of information, as shown in
183 Fig 1A (Supp. Table 5; Supp. Note 6).

184 Beyond the twilight zone, communities of gene clusters

185 The method we developed to group GCs in gene cluster communities (GCCs) (Fig. 2A) reduced
186 the final collection of GCs by 87%, producing 673,601 GCCs (Methods; Fig. 2B; Supp. Note 7).
187 We validated our approach to capture remote homologies between related GCs using two well-
188 known gene families present in our environmental datasets, proteorhodopsins (Olson,
189 Yoshizawa, Boeuf, Iwasaki, & DeLong, 2018) and bacterial ribosomal proteins (Méheust,
190 Burstein, Castelle, & Banfield, 2019). Our dataset contained 64 GCs (12,184 genes) and 3
191 GCCs (Supp Note 8) classified as proteorhodopsin (PR). One *Known* GCC contained 99% of
192 the PR annotated genes (Fig. 2C), except 85 genes taxonomically annotated as viral and
193 assigned to the *PR Supercluster I* (Boeuf, Audic, Brillet-Guéguen, Caron, & Jeanthon, 2015)
194 within two GU communities (five GU gene clusters; Supp. Note 8). For the ribosomal proteins,
195 the results were not so satisfactory. We identified 1,843 GCs (781,579 genes) and 98 GCCs.
196 The number of GCCs is larger than the expected number of ribosomal protein families (16) used
197 for validation. When we use *high-quality* GCs (Supp. Note 8), we get closer to the expected
198 number of GCCs (Fig. 2D). With this subset, we identified 26 GCCs and 145 GCs (1,687
199 genes). The cross-validation of our method against the approach used in Méheust et al.
200 (Méheust et al., 2019) (Supp. Note 9) confirms the intrinsic complexity of analyzing
201 metagenomic data. Both approaches showed a high agreement in the GCCs identified (Supp.
202 Table 9-1). Still, our method inferred fewer GCCs for each of the ribosomal protein families

203 (Supplementary Figure 9-3), coping better with the nuisances of a metagenomic setup, such as

204 incomplete genes (Supp. Table 6).

205

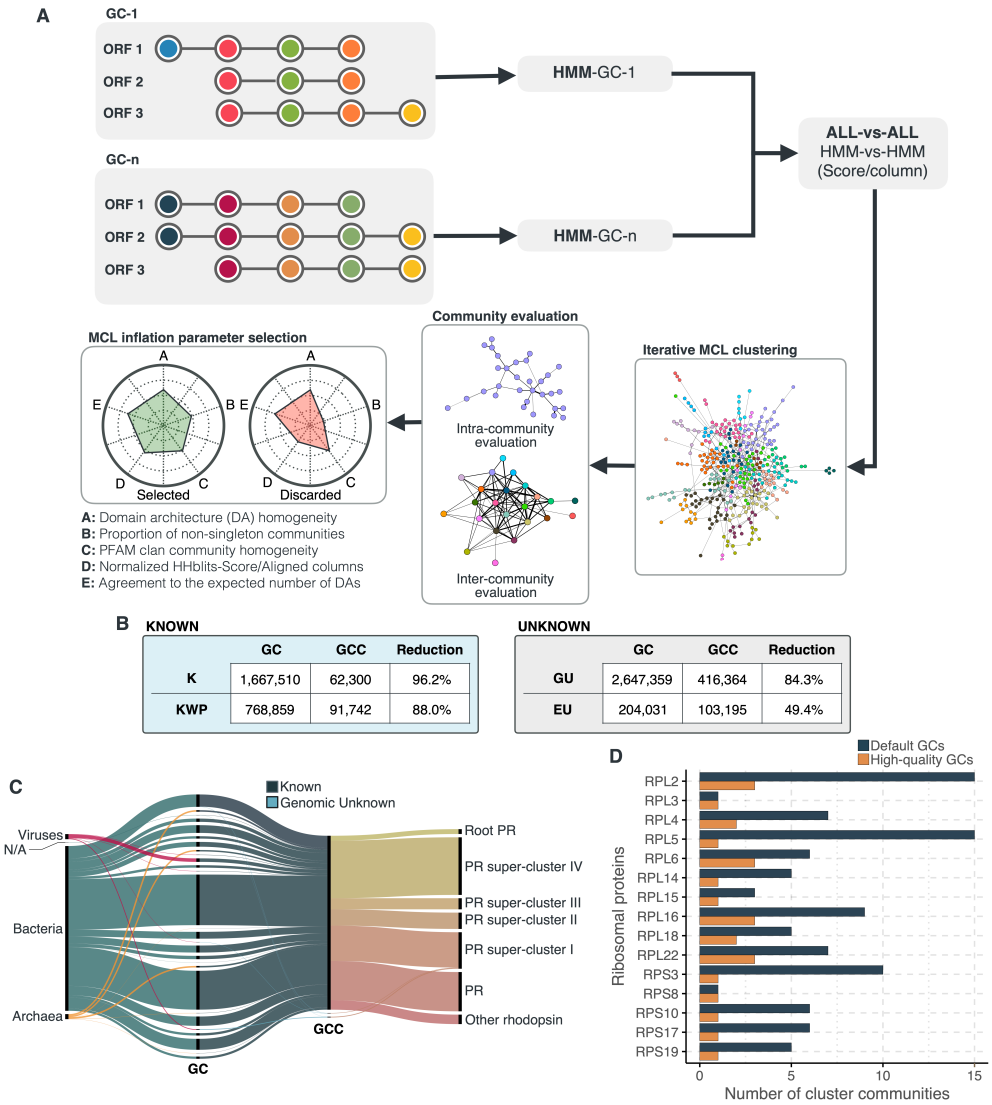

206

207 **Figure 2:** Overview and validation of the workflow to aggregate GCs in communities. (A) We inferred a
208 gene cluster homology network using the results of an all-vs-all HMM gene cluster comparison with
209 HHBLITS. The edges of the network are based on the HHblits-score/Aligned-columns. Communities are
210 identified by an iterative screening of different MCL inflation parameters and evaluated using five different
211 metrics that consider the inter- and intra-community properties. (B) Comparison of the number of GCs
212 and GCCs for each of the functional categories. (C) Validation of the GCCs inference based on the
213 environmental genes annotated as proteorhodopsins. Ribbons in the alluvial plot are genes, and each
214 stacked bar corresponds (from left to right) to the (1) gene taxonomic classification at the domain level,
215 (2) GC membership, (3) GCC membership and (4) MicRhoDE operational classification. (D) Validation of
216 the GCCs inference based on ribosomal proteins based on standard and high-quality GCs.

A smaller but highly diverse unknown coding sequence space

Combining clustering and remote homology searches reduces the extent of the unknown CDS-space compared to what is reported by the traditional genomic and metagenomic analysis approaches (Fig. 3A). Our workflow recruited as much as 71% of genes in human-related metagenomic samples and 65% of the genes in marine metagenomes into the known CDS-space. In both human and marine microbiomes, the genomic unknown fraction showed a similar proportion of genes (21%, Fig. 3A). The number of genes corresponding to EU gene clusters is higher in marine metagenomes; 12% of the genes are part of this GC category. We obtained a comparable result when we evaluated the genes from the GTDB_r86, 75% of bacterial and 64% of archaeal genes were part of the known CDS-space. Archaeal genomes contained more unknowns than those from Bacteria, where 30% of the genes are classified as genomic unknowns in Archaea, and only 20% in Bacteria (Fig. 3A; Supp. Table 7). Our approach allows us to go beyond genes, and for the first time, we can provide a detailed characterization of the CDS-space at the amino acid level. From the 90,128,659,316 amino acids analyzed, the majority of the amino acids in metagenomes (74%) and GTDB_r86 (80%) are in the known CDS-space (Fig. 3B; Supp. Table 7). In both cases, approximately 40% of the amino acids in the known CDS-space were part of a Pfam domain (Fig. 3B; Supp. Table 7). The proportion of amino acids in the unknown CDS-space ranged from 22% in metagenomes and 15% in GTDB_r86. Pfam domains covered only 2% of the amino acids in the unknown CDS-space in both cases. To evaluate the differences between the two CDS-space fractions, we calculated the accumulation rates of GCs and GCCs. For the metagenomic dataset we used 1,264 metagenomes (18,566,675 GCs and 282,580 GCCs) and for the genomic dataset 28,941 genomes (9,586,109 GCs and 496,930 GCCs). The rate of accumulation of unknown GCs was three times higher than the known (2 times for the genomic), and both cases were far from reaching a plateau (Fig. 3C). This is not the case for the GCC accumulation curves (Supp Fig

242 4B), where they reached a plateau. The accumulation rate is largely determined by the number
243 of singletons, especially singletons from EUs (Supp note 11 and Supp. Fig 5). While the
244 accumulation rate of known GCs between marine and human metagenomes is almost identical,
245 there are striking differences for the unknown GCs (Fig. 3D). These differences are maintained
246 even when we remove the virus-enriched samples from the marine metagenomes (Supp Fig
247 4A). Although the marine metagenomes include a large variety of environments, from coastal to
248 the deep sea, the known space remains quite constrained.
249 Despite only including marine and human metagenomes in our database, our coverage of other
250 databases and environments is quite comprehensive, with an overall coverage of 76% (Supp.
251 Note 12). The lowest covered biomes are freshwater, soil and human non-digestive as revealed
252 by the screening of MGnify (Mitchell et al., 2020) (release 2018_09; 11 biomes; 843,535,6116
253 proteins) where we assigned 74% of the MGnify proteins into one of our categories
254 (Supplementary Fig. 6). Furthermore, as a result of this evaluation, we classified 20% of the
255 FunkFams (Wyman et al., 2018) and 44% of the unknowns used by Price et al. (Price et al.,
256 2018) to the known fraction (Supp. Table 12-1).

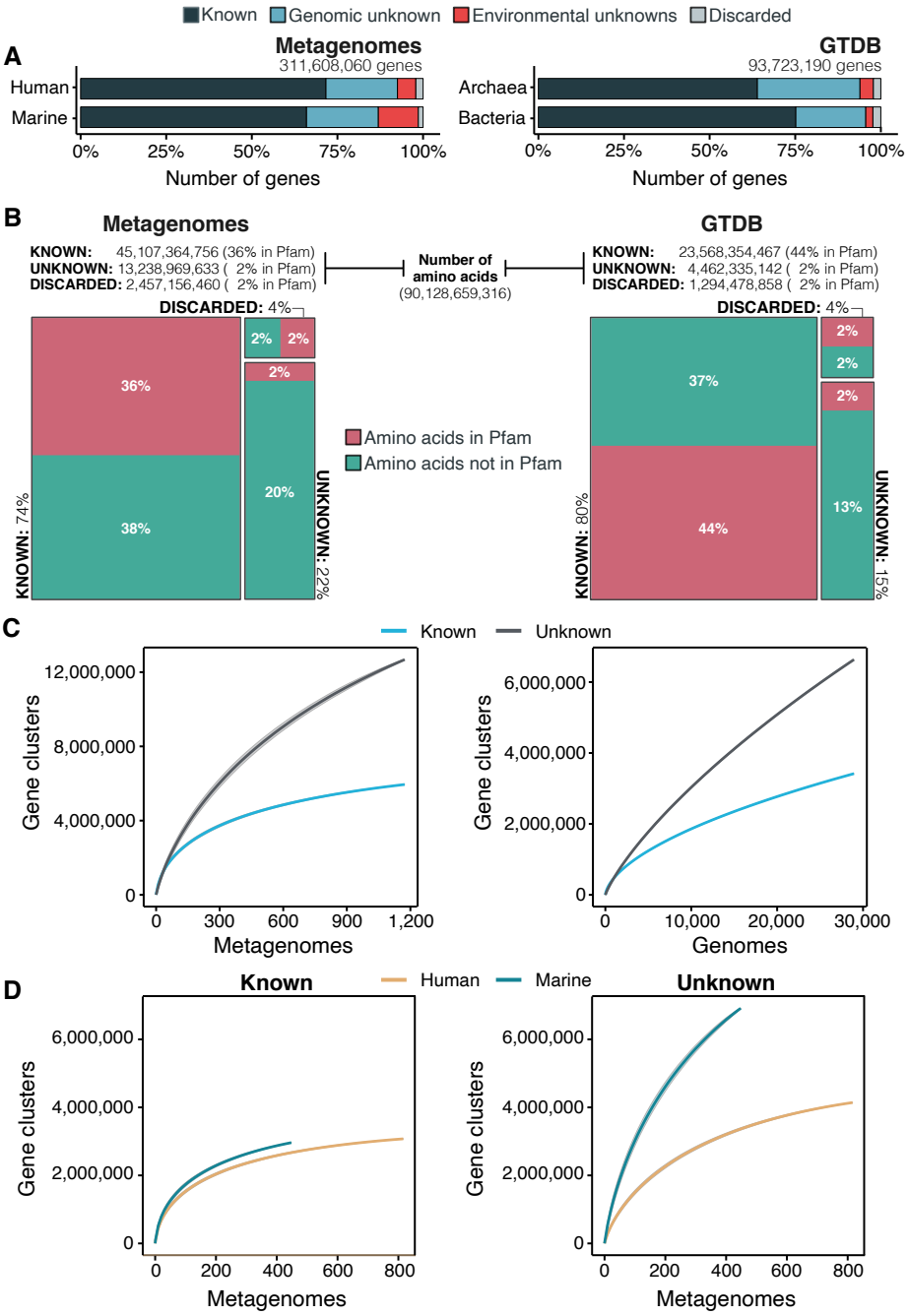

Figure 3: The extent of the known and unknown coding sequence space (A) Proportion of genes in the known and unknown. (B) Amino acid distribution in the known and unknown CDS-space. (C) Accumulation curves for the known and unknown CDS-space at the GC- level for the metagenomic and genomic data. from TARA, MALASPINA, OSD2014 and HMP-I/II projects. (D) Collector curves comparing the human and marine biomes. Colored lines represented the mean of 1000 permutations and shaded in grey the standard deviation. Non-abundant singleton clusters were excluded from the accumulation curves calculation.

The unknown coding sequence space has a limited ecological distribution in human and marine environments

Although the role of the unknown fraction in the environment is still a mystery, the large number of gene counts and abundance observed underlines its inherent ecological relevance (Fig. 4A). In some metagenomes, the genomic unknown fraction can account for more than 40% of the total gene abundance observed (Fig. 4A). The environmental unknown fraction is also relevant in several samples, where singleton GCs are the majority (Fig. 4A). We identified two metagenomes with an unusual composition in terms of environmental unknown singletons. The marine metagenome corresponds to a sample from Lake Faro (OSD42), a meromictic saline with a unique extreme environment where Archaea plays an important role (La Cono et al., 2013). The HMP metagenome (SRS143565) corresponds to a human sample from the right cubital fossa from a healthy female subject. To understand this unusual composition, we should perform further analyses to discard potential technical artifacts like sample contamination. The ratio between the unknown and known GCs revealed that the metagenomes located at the upper left quadrant in Fig. 4B-C are enriched in GCs of unknown function. In human metagenomes, we can distinguish between body sites, with the gastrointestinal tract, where microbial communities are expected to be more diverse and complex, significantly enriched with genomic unknowns. The HMP metagenomes with the largest ratio of unknowns are those samples identified to contain crAssphages (Dubinkina, Ischenko, Ulyantsev, Tyakht, & Alexeev, 2016; Edwards et al., 2019) and HPV viruses (Ma et al., 2014) (Supp. Table 8; Supp. Fig. 7). Consistently, in marine metagenomes (Fig. 4D) we can separate between size fractions, where the highest ratio in genomic and environmental unknowns corresponds to the ones enriched with viruses and giant viruses.

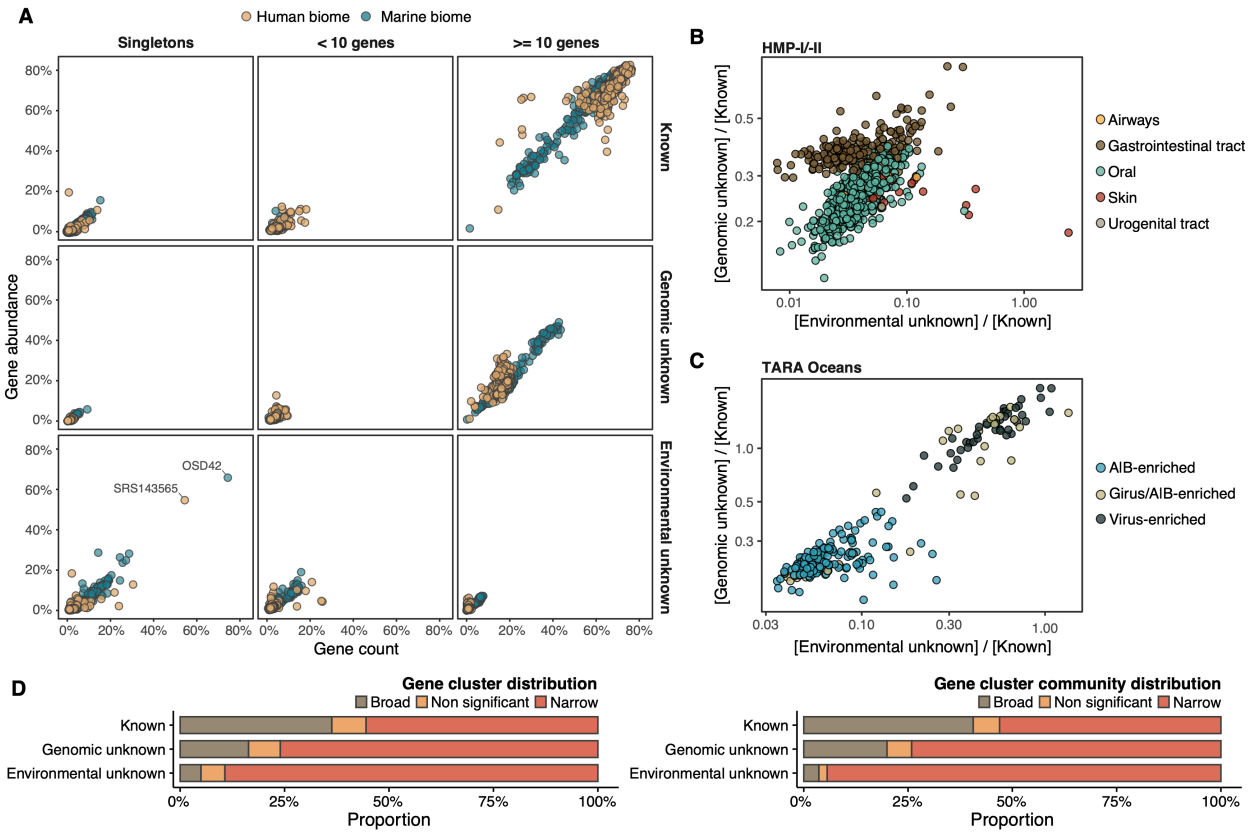

Figure 4: Distribution of the unknown coding sequence space in the human and marine metagenomes (A) Ratio between the proportion of the number of genes and their estimated abundances per cluster category and biome. Columns represented in the facet depicts three cluster categories based on the size of the clusters. (B) Relationship between the ratio of Genomic unknowns and Environmental unknowns in the HMP-I/II metagenomes. Gastrointestinal tract metagenomes are enriched in Genomic unknown coding sequences compared to the other body sites. (C) Relationship between the ratio of Genomic unknowns and Environmental unknowns in the TARA Oceans metagenomes. Girus and virus enriched metagenomes show a higher proportion of both unknown coding sequences (genomic and environmental) than the Archaea|Bacteria enriched fractions. (D) Environmental distribution of GCs and GCCs based on Levin's niche breadth index. We obtained the significance values after generating 100 null gene cluster abundance matrices using the *quasiswap* algorithm.

To complement the previous findings, we performed a large-scale analysis to investigate the GC occurrence patterns in the environment. The narrow distribution of the unknown fraction (Fig. 4D) suggests that these GCs might provide a selective advantage and be necessary to adapt to specific environmental conditions. But the pool of broadly distributed environmental unknowns is the most exciting result. We identified traces of potential ubiquitous organisms left

306 uncharacterized by traditional approaches, as more than 80% of these GCs cannot be
307 associated with a metagenome-assembled genome (MAG) (Supp Table 9, Supp. Note 10).

308 The genomic unknown coding sequence space is lineage-specific

309 With the inclusion of the genomes from GTDB_r86, we have access to a phylogenomic
310 framework that can be used to assess how exclusive is a GC within a lineage (lineage-specifity
311 (Mendler et al., 2019)) and how conserved is a GC across clades (phylogenetic conservation
312 (Martiny, Treseder, & Pusch, 2013)). We identified 781,814 lineage-specific GCs and 464,923
313 phylogenetically conserved ($P < 0.05$) GCs in Bacteria (Supp. Table 10; Supp. Note 13 for
314 Archaea). The number of lineage-specific GCs increases with the Relative Evolutionary
315 Distance (Parks et al., 2018) (Fig. 5A) and differences between the known and the unknown
316 fraction start to be evident at the Family level resulting in 4X more unknown lineage-specific
317 GCs at the Species level. The unknown GCs are more phylogenetically conserved than the
318 known (Fig. 5B, $p < 0.0001$), revealing the importance of the genome's uncharacterized fraction.
319 However, this is not the case for the lineage-specific and phylogenetically conserved GCs,
320 where the unknown GCs are less phylogenetically conserved (Fig. 5B), agreeing with the large
321 number of lineage-specific GCs at Genus and Species level. To discard the possibility that the
322 lineage-specific GCs of unknown function have a viral origin, we screened all GTDB_r86
323 genomes for prophages. We only found 37,163 lineage-specific GCs in prophage genomic
324 regions, being 86% GCs of unknown function. After unveiling the potential relevance of the GCs
325 of unknown function in bacterial genomes, we identified phyla in GTDB_r86 enriched with these
326 types of clusters. A clear pattern emerged when we partitioned the phyla based on the ratio of
327 known to unknown GCs and vice versa (Fig. 5D), the phyla with a larger number of MAGs are
328 enriched in GCs of unknown function Figure 5D. Phyla with a high proportion of non-classified
329 GCs (those discarded during the validation steps) contain a small number of genomes and are
330 primarily composed of MAGs. These groups of phyla highly enriched in unknowns and

represented mainly by MAGs include newly described phyla such as *Cand.* Riflebacteria and *Cand.* Patescibacteria (Anantharaman et al., 2018; Brown et al., 2015; Rinke et al., 2013), both with the largest unknown to known ratio.

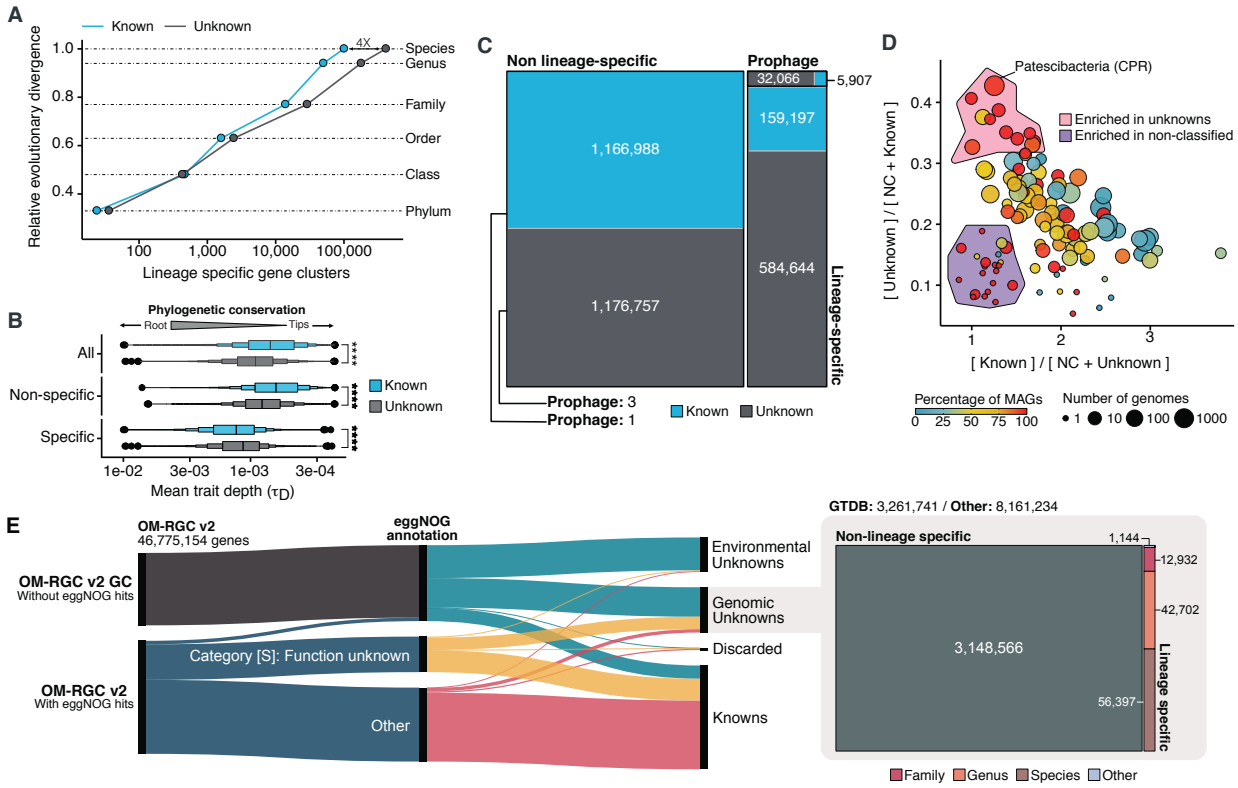

Figure 5: Phylogenomic exploration of the unknown coding sequence space. (A) Distribution of the lineage-specific GCs by taxonomic level. Lineage-specific unknown GCs are more abundant in the lower taxonomic levels (Genus, Species). (B) Phylogenetic conservation of the known and unknown coding sequence space in 27,372 bacterial genomes from GTDB_r86. We observe differences in the conservation between the known and the unknown coding sequence space for lineage- and non-lineage specific GCs (paired Wilcoxon rank-sum test; all p-values < 0.0001). (C) The majority of the lineage-specific clusters are part of the unknown coding sequence space, being a small proportion found in prophages present in the GTDB_r86 genomes. (D) Known and unknown coding sequence space of the 27,732 GTDB_r86 bacterial genomes grouped by bacterial phyla. Phyla are partitioned based on the ratio of known to unknown GCs and vice versa. Phyla enriched in MAGs have higher proportions in GCs of unknown function. Phyla with a high proportion of non-classified clusters (NC; discarded during the validation steps) tend to contain a small number of genomes. (E) The alluvial plot's left side shows the uncharacterized (OM-RGC v2 GC) and characterized (OM-RGC v2) fraction of the gene catalog. The functional annotation is based on the eggNOG annotations provided by Salazar et al.(Salazar et al., 2019). The right side of the alluvial plot shows the new organization of the OM-RGC v2 coding sequence space based on the approach described in this study. The treemap in the right links the metagenomic and genomic space adding context to the unknown fraction of the OM-RGC v2

We demonstrate the possibility of bridging genomic and metagenomic data and simultaneously unifying the known and unknown CDS-space by integrating the new Ocean Microbial Reference Gene Catalog (Salazar et al., 2019) (OM-RGC v2) into our database. We assigned 26,170,875 genes to known GCs, 11,422,975 to genomic unknowns, 8,661,221 to environmental unknown and 520,083 were discarded. From the 11,422,975 genes classified as genomic unknowns, we could associate 3,261,741 to a GTDB_r86 genome and we identified 113,175 as lineage-specific. The alluvial plot in Fig. 5E depicts the new organization of the OM-RGC v2 after being integrated into our framework and how we can provide context to the two original types of unknowns in the OM-RGC (those annotated as category S in eggNOG (Huerta-Cepas et al., 2019) and those without known homologs in the eggNOG database (Salazar et al., 2019)) that can lead to potential experimental targets at the organism level to complement the metatranscriptomic approach proposed by Salazar et al. (Salazar et al., 2019).

A structured coding sequence space augments the interpretation of experimental data

We selected one of the experimental conditions tested in Price et al. (Price et al., 2018) to demonstrate the potential of our approach to augment experimental data. We compared the fitness values in plain rich medium with added Spectinomycin dihydrochloride pentahydrate to the fitness in plain rich medium (LB) in *Pseudomonas fluorescens FW300-N2C3* (Fig. 6A). This antibiotic inhibits protein synthesis and elongation by binding to the bacterial 30S ribosomal subunit and interferes with the peptidyl tRNA translocation. We identified the gene with locus id AO356_08590 that presents a strong phenotype (fitness = -3.1; t = -9.1) and has no known function. This gene belongs to the genomic unknown GC GU_19737823. We can track this GC into the environment and explore the occurrence in the different samples we have in our

database. As expected, the GC is mostly found in non-human metagenomes (Fig. 6B) as *Pseudomonas* are common inhabitants of soil and water environments(Heffernan, Murphy, & Casey, 2009). However, finding this GC also in human-related samples is very interesting due to the potential association of *P. fluorescens* and human disease where Crohn's disease patients develop serum antibodies to this microbe (Scales, Dickson, LiPuma, & Huffnagle, 2014). We can add another layer of information to the selected GC by looking at the associated remote homologs in the GCC GU_c_21103 (Fig. 6C). We identified all the genes in the GTDB_r86 genomes that belong to the GCC GU_c_21103 (Supp. Table 11) and explored their genomic neighborhoods. All members from GU_c_21103 are constrained to the class *Gammaproteobacteria*, and interestingly GU_19737823 is mostly exclusive to the order *Pseudomonadales*. The gene order in the different genomes analyzed is highly conserved, finding GU_19737823 after the *rpsF*::*rpsR* operon and before *rplI*. *rpsF* and *rpsR* encode for 30S ribosomal proteins, the prime target of spectinomycin. The combination of the experimental evidence and the associated data inferred by our approach provides strong support to generate the hypothesis that the gene AO356_08590 might be involved in the resistance to spectinomycin.

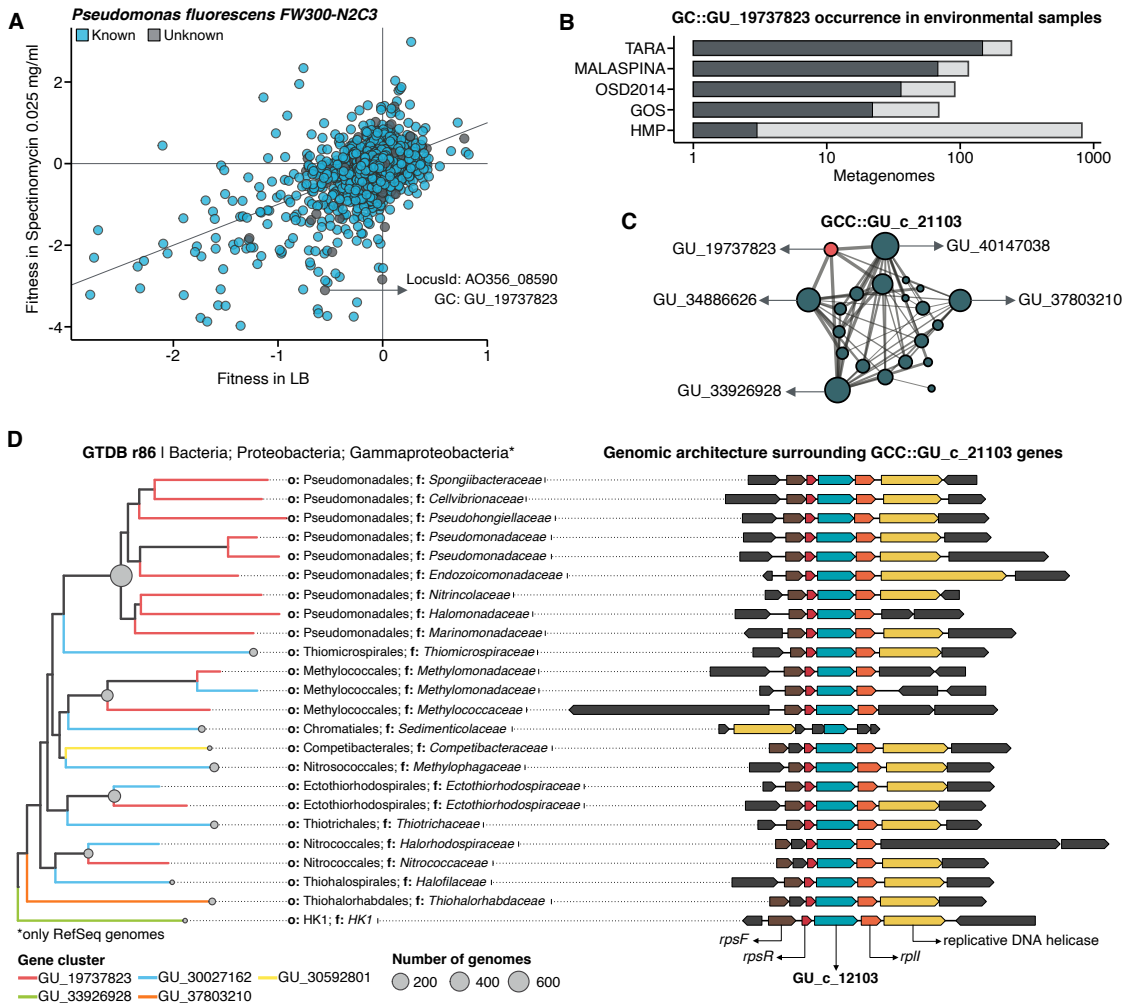

Figure 6: Augmenting experimental data with GCs of unknown function. (A) We used the fitness values from the experiments from Price et al.(Price et al., 2018) to identify genes of unknown function that are important for fitness under certain experimental conditions. The selected gene belongs to the genomic unknown GC GU_19737823 and presents a strong phenotype (fitness = -3.1; t = -9.1) (B) Occurrence of GU_19737823 in the metagenomes used in this study. Darker bars depict the number of metagenomes where the GC is found. (C) GU_19737823 is a member of the GCC GU_c_21103. The network shows the relationships between the different GCs members of the gene cluster community GU_c_21103. The size of the node corresponds to the node degree of each GC. Edge thickness corresponds to the bitscore/column metric. Highlighted in red is GU_19737823. (D) We identified all the genes in the GTDB_r86 genomes that belong to the GCC GU_c_21103 and explored their genomic neighborhoods. GU_c_21103 members were constrained to the class Gammaproteobacteria, and GU_19737823 is mostly exclusive to the order Pseudomonadales. The gene order in the different genomes analyzed is highly conserved, finding GU_19737823 after the *rpsF::rpsR* operon and before *rplI. rpsF* and *rpsR* encode for the *30S ribosomal protein S6* and *30S ribosomal protein S18,* respectively. The GTDB_r86 subtree only shows RefSeq genomes. Branch colors correspond to the different GCs found in GU_c_21103. The bubble plot depicts the number of genomes with a gene that belongs to GU_c_21103.

Discussion

We present a new conceptual framework and computational workflow to unify the known and unknown CDS-space. Using this framework, we performed an in-depth exploration of the microbial unknown CDS-space, demonstrating that we can link the unknown fraction of metagenomic studies to specific genomes and provide a powerful tool for hypothesis generation. During the last years, the microbiome community has established a standard operating procedure(Quince et al., 2017) for analyzing metagenomes that we can briefly summarize into (1) assembly, (2) gene prediction, (3) gene catalog inference, (4) binning, and (5) characterization. Thanks to recent computational developments (Steinegger & Soding, 2017; Steinegger & Söding, 2018), we envisioned an alternative to this workflow to maximize the information used when analyzing genomic and metagenomic data. In addition, we provide a mechanism to reconcile top-down and bottom-up approaches, thanks to the well-structured CDS-space proposed by our framework. AGNOSTOS can create environmental- and organism-specific variations of a seed GC database. Then, it integrates the predicted genes from new genomes and metagenomes and dynamically creates and classifies new GCs with those genes not integrated during the initial step (Fig. 1B). Afterward, the potential functions of the known GCs can be carefully characterized by incorporating them into the traditional workflows.

One of the most appealing characteristics of our approach is that the GCs provide unified groups of homologous genes across environments and organisms indifferently if they belong to the known or unknown CDS-space, and we can contextualize the unknown fraction using this genomic and environmental information. Our combination of partitioning and contextualization features a smaller unknown CDS-space than we expected. On average, for our genomic and metagenomic data, only 30% of the genes fall in the unknown fraction. One hypothesis to reconcile this surprising finding is that the methodologies to identify remotely homologous sequences in large datasets were computationally prohibitive until recently. New methods

438 (Steinegger, Meier, et al., 2019; Steinegger & Soding, 2017), like the ones used in AGNOSTOS,
439 are enabling large scale distant homology searches. Still, one has to apply conservative
440 measures to control the trade-off between specificity and sensitivity to avoid overclassification.
441 We found that most of the coding sequence space at the gene and amino acid level is known,
442 both in genomes and metagenomes. However, it presents a high diversity, as shown in the GC
443 accumulation curves highlighting the vast remaining untapped microbial fraction and its potential
444 importance for niche adaptation owing to its narrow ecological distribution. In a genomic context
445 and after ruling out the effect of prophages, the unknown fraction is predominantly Species'
446 lineage-specific and phylogenetically more conserved than the known fraction, supporting the
447 signal observed in the environmental data emphasizing that we should not ignore the unknown
448 fraction. It is worth noting that the high diversity observed in the unknowns only represents the
449 20% of the amino acids in the CDS-space we analyzed, and only 10% of this unknown amino
450 acid space is part of a Pfam domain (DUF and others). This contrasts with the numbers
451 observed in the known CDS-space, where Pfam domains include 50% of the amino acids. All
452 this evidence combined strengthens the hypothesis that the genes of unknown function,
453 especially the lineage-specific ones, might be associated with the mechanisms of microbial
454 diversification and niche adaptation due to the constant diversification of gene families and the
455 survival of new gene lineages (Francino, 2012; Muller, 2019).
456 Metagenome-assembled genomes are not only unveiling new regions of the microbial universe
457 (42% of the genomes in GTDB_r86), but they are also enriching genes of unknown function in
458 the tree of life. We investigated the unknown CDS-space of *Cand*. Patescibacteria, more
459 commonly known as Candidate Phyla Radiation (CPR), a phylum that has raised considerable
460 interest due to its unusual biology (Brown et al., 2015). We provide a collection of 54,343
461 lineage-specific GCs of unknown function at different taxonomic level resolutions (Supp. Table
462 12; Supp. Note 14), which will be a valuable resource for the CPR advancement research
463 efforts.

464 Our effort to tackle the unknown provides a pathway to unlock a large pool of likely relevant data
465 that remains untapped to analysis and discovery. By identifying a potential target gene of
466 unknown function for antibiotic resistance, we demonstrate the value of our approach and how it
467 can boost insights from model organism experiments. But severe challenges remain, such as
468 the dependence on the quality of the assemblies and their gene predictions, as shown by the
469 analysis of the ribosomal protein GCCs where many of the recovered genes are incomplete.
470 While sequence assembly has been an active area of research (Roumpeka, Wallace,
471 Escalettes, Fotheringham, & Watson, 2017), this has not been the case for gene prediction
472 methods (Roumpeka et al., 2017), which are becoming outdated(Ivanova et al., 2014) and
473 cannot cope with the current amount of data. Alternatives like protein-level assembly
474 (Steinegger, Mirdita, & Söding, 2019) combined with exploring the assembly graphs'
475 neighborhoods (Titus Brown et al., 2018) become very attractive for our purposes. In any case,
476 we still face the challenge of discriminating between real and artifactual singletons (Höps,
477 Jeffryes, & Bateman, 2018). There are currently no methods available to provide a plausible
478 solution and, at the same time, being scalable. We devise a potential solution in the recent
479 developments in unsupervised deep learning methods where they use large corpora of proteins
480 to define a language model *embedding* for protein sequences (Heinzinger et al., 2019). These
481 models could be applied to predict *embeddings* in singletons, which could be clustered or used
482 to determine their coding potential. Another issue is that we might be creating more GCs than
483 expected. We follow a conservative approach to avoid mixing multi-domain proteins in GCs
484 owing to the fragmented nature of the metagenome assemblies that could result in the split of a
485 GC. However, not only splitting can be a problem, but also lumping unrelated genes or GCs
486 owing to the use of remote homologies. Although the inference of GCCs is using very sensitive
487 methods to compare profile HMMs, low sequence diversity in GCs can limit its effectiveness.
488 Moreover, our approach is affected by the presence and propagation of contamination in
489 reference databases, a significant problem in 'omics (Breitwieser, Pertea, Zimin, & Salzberg,

490 2019; Steinegger & Salzberg, 2020). In our case, we only use Pfam as a source for annotation
491 owing to its high-quality and manual curation process. The categorization process of our GCs
492 depends on the information from other databases, and to minimize the potential impact of
493 contamination, we apply methods that weight the annotations of the identified homologs to
494 discriminate if a GC belongs to the known or unknown CDS-space.
495 The results presented here prove that the integration and the analysis of the unknown fraction
496 are possible. We are unveiling a brighter future, not only for microbiome analyses but also for
497 boosting eukaryotic-related studies, thanks to the increasing number of projects, including
498 metatranscriptomic data (Delmont et al., 2020; Vorobev et al., 2020). Furthermore, our work
499 lays the foundations for further developments of clear guidelines and protocols to define the
500 different levels of unknown (Thomas & Segata, 2019) and should encourage the scientific
501 community for a collaborative effort to tackle this challenge.

502 Material and methods

503 Genomic and metagenomic dataset

504 We used a set of 583 marine metagenomes from four of the major metagenomic surveys of the
505 ocean microbiome: Tara Oceans expedition (TARA) (Sunagawa et al., 2015), Malaspina
506 expedition (Duarte, 2015), Ocean Sampling Day (OSD) (Kopf et al., 2015), and Global Ocean
507 Sampling Expedition (GOS) (Rusch et al., 2007). We complemented this set with 1,246
508 metagenomes obtained from the Human Microbiome Project (HMP) phase I and II (Lloyd-Price
509 et al., 2017). We used the assemblies provided by TARA, Malaspina, OSD and HMP projects
510 and the long Sanger reads from GOS (Sanger, Nicklen, & Coulson, 1977). A total of 156M
511 (156,422,969) contigs and 12.8M long-reads were collected (Supp. Table 6).

512 For the genomic dataset, we used the 28,941 prokaryotic genomes (27,372 bacterial and 1,569
513 archaeal) from the Genome Taxonomy Database (Parks et al., 2018) (GTDB) Release 03-RS86
514 (19th August 2018).

515 Computational workflow development

516 We implemented a computation workflow based on Snakemake (Köster, 2018) for the easy
517 processing of large datasets in a reproducible manner. The workflow provides three different
518 strategies to analyze the data. The module *DB-creation* creates the gene cluster database,
519 validates and partitions the gene clusters (GCs) in the main functional categories. The module
520 *DB-update* allows the integration of new sequences (either at the contig or predicted gene level)
521 in the existing gene cluster database. In addition, the workflow has a *profile-search* function to
522 quickly screen samples using the gene cluster PSSM profiles in the database.

523 Metagenomic and genomic gene prediction

524 We used Prodigal (v2.6.3) (Hyatt et al., 2010) in metagenomic mode to predict the genes from
525 the metagenomic dataset. For the genomic dataset, we used the gene predictions provided by
526 Annotree (Mendler et al., 2019), since they were obtained, consistently, with Prodigal v2.6.3.
527 We identified potential spurious genes using the *AntiFam* database (Eberhardt et al., 2012).
528 Furthermore, we screened for '*shadow*' genes using the procedure described in Yooseph et al.
529 (Yooseph, Li, & Sutton, 2008).

530 PFAM annotation

531 We annotated the predicted genes using the *hmmsearch* program from the *HMMER* package
532 (version: 3.1b2) (R. D. Finn, Clements, & Eddy, 2011) in combination with the Pfam database
533 v31 (Robert D. Finn et al., 2016). We kept the matches exceeding the internal gathering

534 threshold and presenting an independent e-value < 1e-5 and coverage > 0.4. In addition, we
535 took into account multi-domain annotations, and we removed overlapping annotations when the
536 overlap is larger than 50%, keeping the ones with the smaller e-value.

537 Determination of the gene clusters

538 We clustered the metagenomic predicted genes using the cascaded-clustering workflow of the
539 MMseqs2 software (Steinegger & Söding, 2018) ("*--cov-mode 0 -c 0.8 --min-seq-id 0.3"*). We
540 discarded from downstream analyses the singletons and clusters with a size below a threshold
541 identified after applying a broken-stick model (Bennett, 1996). We integrated the genomic data
542 into the metagenomic cluster database using the "DB-update" module of the workflow. This
543 module uses the *clusterupdate* module of MMseqs2 (Steinegger & Soding, 2017), with the same
544 parameters used for the metagenomic clustering.

545 Quality-screening of gene clusters

546 We examined the GCs to ensure their high intra-cluster homogeneity. We applied two
547 methodologies to validate their cluster sequence composition and functional annotation
548 homogeneity. We identified non-homologous sequences inside each cluster combining the
549 identification of a new cluster representative sequence via a sequence similarity network (SSN)
550 analysis, and the investigation of intra-cluster multiple sequence alignments (MSAs), given the
551 new representative. Initially, we generated an SSN for each cluster, using the semi-global
552 alignment methods implemented in *PARASAIL* (Daily, 2016) (version 2.1.5). We trimmed the
553 SSN using a custom algorithm (Chafee et al., 2018; Žure, Fernandez-Guerra, Munn, & Harder,
554 2017) that removes edges while maintaining the network structural integrity and obtaining the
555 smallest connected graph formed by a single component. Finally, the new cluster representative
556 was identified as the most central node of the trimmed SSN by the eigenvector centrality
557 algorithm, as implemented in igraph (Csardi & Nepusz, 2006). After this step, we built a multiple

558 sequence alignment for each cluster using *FAMSA* (Deorowicz, Debudaj-Grabysz, & Gudyś,
559 2016) (version 1.1). Then, we screened each cluster-MSA for non-homologous sequences to
560 the new cluster representative. Owing to computational limitations, we used two different
561 approaches to evaluate the cluster-MSAs. We used *LEON-BIS* (Vanhoutreve et al., 2016) for
562 the clusters with a size ranging from 10 to 1,000 genes and OD-SEQ (Jehl, Sievers, & Higgins,
563 2015) for the clusters with more than 1,000 genes. In the end, we applied a broken-stick model
564 (Bennett, 1996) to determine the threshold to discard a cluster.
565 The predicted genes can have multi-domain annotations in different orders, therefore to validate
566 the consistency of intra-cluster Pfam annotations, we applied a combination of w-shingling
567 (Broder, 1997) and Jaccard similarity. We used w-shingling (k-shingle = 2) to group consecutive
568 domain annotations as a single object. We measured the homogeneity of the *shingle sets* (sets
569 of domains) between genes using the Jaccard similarity and reported the median similarity
570 value for each cluster. Moreover, we took into consideration the Clan membership of the Pfam
571 domains and that a gene might contain N-, C- and M-terminal domains for the functional
572 homogeneity validation. We discarded clusters with a median similarity < 1.
573 After the validation, we refined the gene cluster database removing the clusters identified to be
574 discarded and the clusters containing ≥ 30% *shadow genes*. Lastly, we removed the single
575 shadow, spurious and non-homologous genes from the remaining clusters (Supplementary Note
576 2).

577 Remote homology classification of gene clusters

578 To partition the validated GCs into the four main categories, we processed the set of GCs
579 containing Pfam annotated genes and the set of not annotated GCs separately. For the
580 annotated GCs, we inferred a consensus protein domain architecture (DA) (an ordered
581 combination of protein domains) for each annotated gene cluster. To identify each gene cluster
582 consensus DA, we created directed acyclic graphs connecting the Pfam domains based on their

583 topological order on the genes using *igraph* (Csardi & Nepusz, 2006). We collapsed the
584 repetitions of the same domain. Then we used the gene completeness as a positive-weighting
585 value for the selection of the cluster consensus DA. Within this step, we divided the GCs into
586 "Knowns" (Known) if annotated to at least one Pfam domains of known function (DKFs) and
587 "Genomic unknowns" (GU) if annotated entirely to Pfam domains of unknown function (DUFs).
588 We aligned the sequences of the non-annotated GCs with FAMSA (Deorowicz et al., 2016) and
589 obtained cluster consensus sequences with the *hhconsensus* program from *HH-SUITE*
590 (Steinegger, Meier, et al., 2019). We used the cluster consensus sequences to perform a
591 nested search against the UniRef90 database (release 2017_11) (The UniProt Consortium,
592 2017) and NCBI *nr* database (release 2017_12) (NCBI Resource Coordinators, 2018) to retrieve
593 non-Pfam annotations with *MMSeqs2* (Steinegger & Soding, 2017) ("*-e 1e-05 --cov-mode 2 -c*
594 *0.6"*). We kept the hits within 60% of the Log(best-e-value) and searched the annotations for
595 any of the terms commonly used to define proteins of unknown function (Supp. Table 12). We
596 used a quorum majority voting approach to decide if a gene cluster would be classified as
597 *Genomic Unknown* or *Known without Pfams* based on the annotations retrieved. We searched
598 the consensus sequences without any homologs in the UniRef90 database against NCBI *nr*. We
599 applied the same approach and criteria described for the first search. Ultimately, we classified
600 as *Environmental Unknown* those GCs whose consensus sequences did not align with any of
601 the NCBI *nr* entries.
602 In addition, we developed some conservative measures to control the trade-off between
603 specificity and sensitivity for the remote homology searches such as (1) a modification of the
604 algorithm described in Hingamp et al. (Hingamp et al., 2013) to get a confident group of
605 homologs to determine if a query protein is known or unknown by a quorum majority voting
606 approach (Supp Note 3); (2) strict parameters in terms of iterations, bidirectional coverage and
607 probability thresholds for the HHblits alignments to minimize the inclusion of non-homologous

608 sequences; and (3) avoid providing annotations for our gene clusters, as we believe that
609 annotation should be a careful process done on a smaller scale and with experimental context.

610 Gene cluster remote homology refinement

611 We refined the *Environmental Unknown* GCs to ensure the lack of any characterization by
612 searching for remote homologies in the Uniclust database (release 30_2017_10) using the
613 HMM/HMM alignment method *HHblits* (Remmert, Biegert, Hauser, & Söding, 2012). We created
614 the HMM profiles with the *hhmake* program from the *HH-SUITE* (Steinegger, Meier, et al.,
615 2019). We only accepted those hits with an *HHblits-probability* ≥ 90% and we re-classified them
616 following the same majority vote approach as previously described. The clusters with no hits
617 remained as the refined set of EUs. We applied a similar refinement approach to the KWP
618 clusters to identify GCs with remote homologies to Pfam protein domains. The KWP HMM
619 profiles were searched against the Pfam *HH-SUITE* database (version 31), using *HHblits*. We
620 accepted hits with a probability ≥ 90% and a target coverage > 60% and removed overlapping
621 domains as described earlier. We moved the KWP with remote homologies to known Pfams to
622 the Known set, and those showing remote homologies to Pfam DUFs to the GUs. The clusters
623 with no hits remained as the refined set of KWP.

624 Gene cluster characterization

625 To retrieve the taxonomic composition of our clusters we applied the *MMseqs2 taxonomy*
626 program (version: b43de8b7559a3b45c8e5e9e02cb3023dd339231a), which allows computing
627 the lowest common ancestor through the implementation of the 2bLCA protocol (Hingamp et al.,
628 2013). We searched all cluster genes against UniProtKB (release of January 2018) (UniProt
629 Consortium, 2018) using the following parameters "*-e 1e-05 --cov-mode 0 -c 0.6"*. We parsed
630 the results to keep only the hits within 60% of the log10(best-e-value). To retrieve the taxonomic
631 lineages, we used the R package *CHNOSZ* (Dick, 2008). We measured the intra-cluster

632 taxonomic admixture by applying the *entropy.empirical()* function from the *entropy* R package
633 (Hausser & Strimmer, 2008). This function estimates the Shannon entropy based on the
634 different taxonomic annotation frequencies. For each cluster, we also retrieved the cluster
635 consensus taxonomic annotation, which we defined as the taxonomic annotation of the majority
636 of the genes in the cluster.
637 In addition to the taxonomy, we evaluated the clusters' level of darkness and disorder using the
638 Dark Proteome Database (DPD) (Perdigão et al., 2017) as reference. We searched the cluster
639 genes against the DPD, applying the MMseqs2 search program (Steinegger & Soding, 2017)
640 with "*-e 1e-20 --cov-mode 0 -c 0.6*". For each cluster, we then retrieved the mean and the
641 median level of darkness, based on the gene DPD annotations.

642 High-quality clusters

643 We defined a subset of high-quality clusters based on the completeness of the cluster genes
644 and their representatives. We identified the minimum required percentage of complete genes
645 per cluster by a broken-stick model (Bennett, 1996) applied to the percentage distribution. Then,
646 we selected the GCs found above the threshold and with a complete representative.

647 A set of non-redundant domain architectures

648 We estimated the number of potential domain architectures present in the *Known* GCs taking
649 into account the large proportion of fragmented genes in the metagenomic dataset and that
650 could inflate the number of potential domain architectures. To identify fragments of larger
651 domain architecture, we took into account their topological order in the genes. To reduce the
652 number of comparisons, we calculated the pairwise string cosine distance (q-gram = 3) between
653 domain architectures and discarded the pairs that were too divergent (cosine distance ≥ 0.9).
654 We collapsed a fragmented domain architecture to the larger one when it contained less than
655 75% of complete genes.

656 ## Inference of gene cluster communities

657 We aggregated distant homologous GCs into GCCs. The community inference approach
658 combined an all-vs-all HMM gene cluster comparison with Markov Cluster Algorithm (MCL) (van
659 Dongen & Abreu-Goodger, 2012) community identification. We started performing the inference
660 on the Known GCs to use the Pfam DAs as constraints. We aligned the gene cluster HMMs
661 using HHblits (Remmert et al., 2012) (-n 2 -Z 10000000 -B 10000000 -e 1) and we built a
662 homology graph using the cluster pairs with probability ≥ 50% and bidirectional coverage > 60%.
663 We used the ratio between HHblits-bitscore and aligned-columns as the edge weights (Supp.
664 Note 9). We used MCL (van Dongen & Abreu-Goodger, 2012) (v. 12-068) to identify the
665 communities present in the graph. We developed an iterative method to determine the optimal
666 MCL inflation parameter that tries to maximize the relationship of five intra-/inter-community
667 properties: (1) the proportion of MCL communities with one single DA, based on the consensus
668 DAs of the cluster members; (2) the ratio of MCL communities with more than one cluster; (3)
669 the proportion of MCL communities with a PFAM clan entropy equal to 0; (4) the intra-
670 community HHblits-score/Aligned-columns score (normalized by the maximum value); and (5)
671 the number of MCL communities, which should, in the end, reflect the number of non-redundant
672 DAs. We iterated through values ranging from 1.2 to 3.0, with incremental steps of 0.1. During
673 the inference process, some of the GCs became orphans in the graph. We applied a three-step
674 approach to assigning a community membership to these GCs. First, we used less stringent
675 conditions (probability ≥ 50% and coverage >= 40%) to find homologs in the already existing
676 GCCs. Then, we ran a second iteration to find secondary relationships between the newly
677 assigned GCs and the missing ones. Lastly, we created new communities with the remaining
678 GCs. We repeated the whole process with the other categories (KWP, GU and EU), applying
679 the optimal inflation value found for the Known (2.2 for metagenomic and 2.5 for genomic data).

680 # Gene cluster communities validation

681 We tested the biological significance of the GCCs using the phylogeny of proteorhodopsin
682 (Boeuf et al., 2015) (PR). We used the proteorhodopsin HMM profiles (Olson et al., 2018) to
683 screen the marine metagenomic datasets using *hmmsearch* (version 3.1b2) (R. D. Finn et al.,
684 2011). We kept the hits with a coverage > 0.4 and e-value <= 1e-5. We removed identical
685 duplicates from the sequences assigned to PR with CD-HIT (W. Li & Godzik, 2006) (v4.6) and
686 cleaned from sequences with less than 100 amino acids. To place the identified PR sequences
687 into the MicRhode (Boeuf et al., 2015) PR tree first, we optimized the initial tree parameters and
688 branch lengths with RAxML (v8.2.12) (Stamatakis, 2014). We used PaPaRA (v2.5) (Berger &
689 Stamatakis, 2012) to incrementally align the query PR sequences against the MicRhode PR
690 reference alignment and *pplacer* (Matsen, Kodner, & Armbrust, 2010) (v1.1.alpha19-0-g807f6f3)
691 to place the sequences into the tree. Finally, we assigned the query PR sequences to the
692 MicRhode PR Superclusters based on the phylogenetic placement. We further investigated the
693 GCs annotated as viral (196 genes, 14 GC) comparing them to the six newly discovered viral
694 PRs (Needham et al., 2019) using Parasail (Daily, 2016) (-a sg_stats_scan_sse2_128_16 -t 8 -c
695 1 -x). As an additional evaluation, we investigated the distributions of standard GCCs and HQ
696 GCCs within ribosomal protein families. We obtained the ribosomal proteins used for the
697 analysis combining the set of 16 ribosomal proteins from Méheust et al. (Méheust et al., 2019)
698 and those contained in the collection of bacterial single-copy genes of Anvi'o (Murat Eren et al.,
699 2015). Also, for the ribosomal proteins, we compared the outcome of our method to the one
700 proposed by Méheust et al. (Méheust et al., 2019) (Supp. Note 9).

701 ## Metagenomic sample selection for downstream analyses

702 For the subsequent ecological analyses, we selected those metagenomes with a number of
703 genes larger or equal to the first quartile of the distribution of all the metagenomic gene counts.
704 (Supp. Table 13).

705 ## Gene cluster abundance profiles in genomes and metagenomes

706 We estimated abundance profiles for the metagenomic cluster categories using the read
707 coverage to each predicted gene as a proxy for abundance. We calculated the coverage by
708 mapping the reads against the assembly contigs using the *bwa-mem* algorithm from *BWA*
709 *mapper* (H. Li & Durbin, 2010). Then, we used *BEDTOOLS* (Quinlan & Hall, 2010), to find the
710 intersection of the gene coordinates to the assemblies, and normalize the per-base coverage by
711 the length of the gene. We calculated the cluster abundance in a sample as the sum of the
712 cluster gene abundances in that sample, and the cluster category abundance in a sample as the
713 sum of the cluster abundances. We obtained the proportions of the different gene cluster
714 categories applying a total-sum-scaling normalization. For the genomic abundance profiles, we
715 used the number of genes in the genomes and normalized by the total gene counts per
716 genome.

717 ## Rate of genomic and metagenomic gene clusters accumulation

718 We calculated the cumulative number of known and unknown GCs as a function of the number
719 of metagenomes and genomes. For each metagenome count, we generated 1000 random sets,
720 and we calculated the number of GCs and GCCs recovered. For this analysis, we used 1,246
721 HMP metagenomes and 358 marine metagenomes (242 from TARA and 116 from Malaspina).
722 We repeated the same procedure for the genomic dataset. We removed the singletons from the
723 metagenomic dataset with an abundance smaller than the mode abundance of the singletons

724 that got reclassified as good-quality clusters after integrating the GTDB data to minimize the
725 impact of potential spurious singletons. To complement those analyses, we evaluated the
726 coverage of our dataset by searching seven different state-of-the-art databases against our set
727 of metagenomic GC HMM profiles (Supp. Note 12).
728

729 Occurrence of gene clusters in the environment

730 We used 1,264 metagenomes from the TARA Oceans, MALASPINA Expedition, OSD2014 and
731 HMP-I/II to explore the properties of the unknown CDS-space in the environment. We applied
732 the Levins Niche Breadth (NB) index (Levins, 1966) to investigate the GCs and GCCs
733 environmental distributions. We removed the GCs and cluster communities with a mean relative
734 abundance < 1e-5. We followed a divide-and-conquer strategy to avoid the computational
735 burden of generating the null-models to test the significance of the distributions owing to the
736 large number of metagenomes and GCs. First, we grouped similar samples based on the gene
737 cluster content using the Bray-Curtis dissimilarity(Bray, Roger Bray, & Curtis, 1957) in
738 combination with the *Dynamic Tree Cut* (Langfelder, Zhang, & Horvath, 2008) R package. We
739 created 100 random datasets picking up one random sample from each group. For each of the
740 100 random datasets, we created 100 random abundance matrices using the *nullmodel* function
741 of the *quasiswap* count method (Miklós & Podani, 2004). Then we calculated the *observed* NB
742 and obtained the 2.5% and 97.5% quantiles based on the randomized sets. We compared the
743 observed and quantile values for each gene cluster and defined it to have a *Narrow distribution*
744 when the *observed* was smaller than the 2.5% quantile and to have a *Broad distribution* when it
745 was larger than the 97.5% quantile. Otherwise, we classified the cluster as *Non-significant*
746 (Salazar et al., 2015). We used a majority voting approach to get a consensus distribution
747 classification based on the ten random datasets.

Identification of prophages in genomic sequences

We used PhageBoost (https://github.com/ku-cbd/PhageBoost/) to find gene regions in the microbial genomes that result in high viral signals against the overall genome signal. We set the following thresholds to consider a region prophage: minimum of 10 genes, maximum 5 gaps, single-gene probability threshold 0.9. We further smoothed the predictions using Parzen rolling windows of 20 periods and looked at the smoothed probability distribution across the genome. We disregarded regions that had a summed smoothed probability less than 0.5, and those regions that did differ from the overall population of the genes in a genome by using Kruskal–Wallis rank test (p-value 0.001).

Lineage-specific gene clusters

We used the F1-score developed for AnnoTree (Mendler et al., 2019) to identify the lineage-specific GCs and to which rank they are specific. Following similar criteria to the ones used in Mendler et al. (Mendler et al., 2019), we considered a gene cluster to be lineage-specific if it is present in less than half of all genomes and at least 2 with F1-score > 0.95.

Phylogenetic conservation of gene clusters

We calculated the phylogenetic conservation (τD) of each gene cluster using the *consenTRAIT* (Martiny et al., 2013) function implemented in the R package *castor* (Martiny et al., 2013). We used a paired Wilcoxon rank-sum test to compare the average τD values for lineage-specific and non-specific GCs.

Evaluation of the OM-RGC v2 uncharacterized fraction

We integrated the 46,775,154 genes from the second version of the TARA Ocean Microbial Reference Gene Catalog (OM-RGC v2) (Salazar et al., 2019) into our cluster database using

770 the same procedure as for the genomic data. We evaluated the uncharacterized fraction and the
771 genes classified into the eggNOG (Huerta-Cepas et al., 2019) category S within the context of
772 our database.

773 Augmenting RB-TnSeq experimental data

774 We searched the 37,684 genes of unknown function associated with mutant phenotypes from
775 Price et al. (Price et al., 2018) against our gene cluster profiles. We kept the hits with e-value ≤
776 1e-20 and a query coverage > 60%. Then we filtered the results to keep the hits within 90% of
777 the Log(best-e-value), and we used a majority vote function to retrieve the consensus category
778 for each hit. Lastly, we selected the best-hits based on the smallest e-value and the largest
779 query and target coverage values. We used the fitness values from the RB-TnSeq experiments
780 from Price et al. to identify genes of unknown function that are important for fitness under
781 certain experimental conditions.

782 Availability of data and materials

783 The code used for the analyses in the manuscript is available at https://github.com/functional-
784 dark-side/functional-dark-side.github.io/tree/master/scripts. The code to recreate the figures is
785 available at https://github.com/functional-dark-side/vanni_et_al-figures. Detailed descriptions of
786 the different methods and results of this manuscript are available at
787 https://dark.metagenomics.eu. The workflow AGNOSTOS is available at
788 https://github.com/functional-dark-side/agnostos-wf, and its database can be downloaded from
789 https://doi.org/10.6084/m9.figshare.12459056.
790
791

Acknowledgements

The authors thankfully acknowledge the computer resources at MareNostrum and the technical support provided by Barcelona Supercomputing Center (RES-AECT-2014-2-0085), the BMBF-funded de.NBI Cloud within the German Network for Bioinformatics Infrastructure (de.NBI) (031A537B, 031A533A, 031A538A, 031A533B, 031A535A, 031A537C, 031A534A, 031A532B), the University of Oxford Advanced Research Computing (http://dx.doi.org/10.5281/zenodo.22558) and the MARBITS bioinformatics core at ICM-CSIC. CV was supported by the Max Planck Society. AFG received funding from the European Union's Horizon 2020 research and innovation program Blue Growth: Unlocking the potential of Seas and Oceans under grant agreement no. 634486 (project acronym INMARE). AM was supported by the Biotechnology and Biological Sciences Research Council [BB/M011755/1, BB/R015228/1] and RDF by the European Molecular Biology Laboratory core funds. EOC was supported by project INTERACTOMA RTI2018-101205-B-I00 from the Spanish Agency of Science MICIU/AEI. SGA and PS received additional funding by the project MAGGY (CTM2017-87736-R) from the Spanish Ministry of Economy and Competitiveness. The Malaspina 2010 Expedition was supported by the Spanish Ministry of Economy and Competitiveness (MINECO) through the Consolider-Ingenio program (ref. CSD2008-00077). The authors thank Johannes Söding and Alex Bateman for helpful discussions.

Contributions

CV, MSS and AF-G performed the analyses and wrote the computational workflow. MS assisted with the clustering and remote homology searches. KS helped with the identification of prophages in genomic sequences. PLB and AB provided feedback and assisted with the ecological analyses. RDF and AM provided feedback and information on the MGnify and Pfam

816 databases. CMD, PS and SGA provided the Malaspina metagenomes. TOD and AME analyzed
817 data in the context of metagenome-assembled genomes. AF-G conceived the study and
818 supervised the work. CV and AF-G wrote the manuscript. All authors read, edited and approved
819 the final manuscript.

820 Competing Interests

821 The authors declare no competing interests.

References

Almeida, A., Mitchell, A. L., Boland, M., Forster, S. C., Gloor, G. B., Tarkowska, A., … Finn, R. D. (2019). A new genomic blueprint of the human gut microbiota. *Nature*, *568*(7753), 499–504.

Almeida, A., Nayfach, S., Boland, M., Strozzi, F., Beracochea, M., Shi, Z. J., … Finn, R. D. (2020). A unified catalog of 204,938 reference genomes from the human gut microbiome. *Nature Biotechnology*. doi:10.1038/s41587-020-0603-3

Anantharaman, K., Hausmann, B., Jungbluth, S. P., Kantor, R. S., Lavy, A., Warren, L. A., … Banfield, J. F. (2018). Expanded diversity of microbial groups that shape the dissimilatory sulfur cycle. *The ISME Journal*, *12*(7), 1715–1728.

Arnold, F. H. (1998). Design by Directed Evolution. *Accounts of Chemical Research*, *31*(3), 125–131.

Arnold, F. H. (2018). Directed Evolution: Bringing New Chemistry to Life. *Angewandte Chemie* , *57*(16), 4143–4148.

Bateman, A., Coggill, P., & Finn, D. R. (2010). DUFs: Families in search of function. *Acta Crystallographica. Section F, Structural Biology and Crystallization Communications*, *66*(10), 1148–1152.

Bennett, K. D. (1996). Determination of the number of zones in a biostratigraphical sequence. *The New Phytologist*, *132*(1), 155–170.

Berger, S. A., & Stamatakis, A. (2012). PaPaRa 2.0: a vectorized algorithm for probabilistic phylogeny-aware alignment extension. *Heidelberg Institute for Theoretical Studies, Http://Sco. h-Its. Org/Exelixis/Publica Tions. Html. Exelixis-RRDR-2012-2015*. Retrieved from https://cme.h-its.org/exelixis/pubs/Exelixis-RRDR-2012-5.pdf

Bernard, G., Pathmanathan, J. S., Lannes, R., Lopez, P., & Bapteste, E. (2018). Microbial Dark Matter Investigations: How Microbial Studies Transform Biological Knowledge and

Empirically Sketch a Logic of Scientific Discovery. *Genome Biology and Evolution*, *10*(3), 707–715.

Bileschi, M. L., Belanger, D., Bryant, D., Sanderson, T., Carter, B., Sculley, D., … Colwell, L. J. (2019). Using Deep Learning to Annotate the Protein Universe (p. 626507). doi:10.1101/626507

Bitard-Feildel, T., & Callebaut, I. (2017). Exploring the dark foldable proteome by considering hydrophobic amino acids topology. *Scientific Reports*, *7*, 41425.

Boeuf, D., Audic, S., Brillet-Guéguen, L., Caron, C., & Jeanthon, C. (2015). MicRhoDE: a curated database for the analysis of microbial rhodopsin diversity and evolution. *Database: The Journal of Biological Databases and Curation*, *2015*. doi:10.1093/database/bav080

Brandenberg, O. F., Fasan, R., & Arnold, F. H. (2017). Exploiting and engineering hemoproteins for abiological carbene and nitrene transfer reactions. *Current Opinion in Biotechnology*, *47*, 102–111.

Bray, J. R., Roger Bray, J., & Curtis, J. T. (1957). An Ordination of the Upland Forest Communities of Southern Wisconsin. *Ecological Monographs*, Vol. 27, pp. 325–349. doi:10.2307/1942268

Breitwieser, F. P., Pertea, M., Zimin, A., & Salzberg, S. L. (2019). Human contamination in bacterial genomes has created thousands of spurious proteins. *Genome Research*. doi:10.1101/gr.245373.118

Broder, A. Z. (1997). On the resemblance and containment of documents. *Proceedings. Compression and Complexity of SEQUENCES 1997 (Cat. No. 97TB100171)*, 21–29. IEEE.

Brown, C. T., Hug, L. A., Thomas, B. C., Sharon, I., Castelle, C. J., Singh, A., … Banfield, J. F. (2015). Unusual biology across a group comprising more than 15% of domain Bacteria. *Nature*, *523*(7559), 208–211.

Brum, J. R., Cesar Ignacio-Espinoza, J., Kim, E.-H., Trubl, G., Jones, R. M., Roux, S., … Sullivan, M. B. (2016). Illuminating structural proteins in viral “dark matter” with metaproteomics. *Proceedings of the National Academy of Sciences of the United States of America*, *113*(9), 2436–2441.

Buttigieg, L. P., Hankeln, W., Kostadinov, I., Kottmann, R., Yilmaz, P., Duhaime, B. M., & Gl??ckner, O. F. (2013). Ecogenomic Perspectives on Domains of Unknown Function: Correlation-Based Exploration of Marine Metagenomes. *PloS One*, *8*(3).

Carradec, Q., Pelletier, E., Da Silva, C., Alberti, A., Seeleuthner, Y., Blanc-Mathieu, R., … Wincker, P. (2018). A global ocean atlas of eukaryotic genes. *Nature Communications*, *9*(1), 373.

Chafee, M., Fernàndez-Guerra, A., Buttigieg, P. L., Gerdts, G., Eren, A. M., Teeling, H., & Amann, R. I. (2018). Recurrent patterns of microdiversity in a temperate coastal marine environment. *The ISME Journal*, *12*(1), 237–252.

Chen, I.-M. A., Chu, K., Palaniappan, K., Pillay, M., Ratner, A., Huang, J., … Kyrpides, N. C. (2019). IMG/M v.5.0: an integrated data management and comparative analysis system for microbial genomes and microbiomes. *Nucleic Acids Research*, *47*(D1), D666–D677.

Cross, K. L., Campbell, J. H., Balachandran, M., Campbell, A. G., Cooper, S. J., Griffen, A., … Podar, M. (2019). Targeted isolation and cultivation of uncultivated bacteria by reverse genomics. *Nature Biotechnology*, *37*(11), 1314–1321.

Csardi, G., & Nepusz, T. (2006). The igraph software package for complex network research. *InterJournal*, p. 1695. Retrieved from http://igraph.org

Daily, J. (2016). Parasail: SIMD C library for global, semi-global, and local pairwise sequence alignments. *BMC Bioinformatics*, *17*(1), 81–81.

Delmont, T. O., Gaia, M., Hinsinger, D. D., Fremont, P., Guerra, A. F., Murat Eren, A., … Jaillon, O. (2020). Functional repertoire convergence of distantly related eukaryotic plankton lineages revealed by genome-resolved metagenomics (p. 2020.10.15.341214).

doi:10.1101/2020.10.15.341214

Deorowicz, S., Debudaj-Grabysz, A., & Gudyś, A. (2016). FAMSA: Fast and accurate multiple sequence alignment of huge protein families. *Scientific Reports*, *6*(1), 33964–33964.

Dick, J. M. (2008). Calculation of the relative metastabilities of proteins using the CHNOSZ software package. *Geochemical Transactions*, *9*, 10.

Duarte, C. M. (2015). Seafaring in the 21St Century: The Malaspina 2010 Circumnavigation Expedition. *Limnology and Oceanography Bulletin*, *24*(1), 11–14.

Dubinkina, V. B., Ischenko, D. S., Ulyantsev, V. I., Tyakht, A. V., & Alexeev, D. G. (2016). Assessment of k-mer spectrum applicability for metagenomic dissimilarity analysis. *BMC Bioinformatics*, Vol. 17. doi:10.1186/s12859-015-0875-7

Eberhardt, R. Y., Haft, D. H., Punta, M., Martin, M., O'Donovan, C., & Bateman, A. (2012). AntiFam: a tool to help identify spurious ORFs in protein annotation. *Database*, *2012*(0), bas003–bas003.

Edwards, R. A., Vega, A. A., Norman, H. M., Ohaeri, M., Levi, K., Dinsdale, E. A., … Dutilh, B. E. (2019). Global phylogeography and ancient evolution of the widespread human gut virus crAssphage. *Nature Microbiology*, *4*(10), 1727–1736.

Eloe-Fadrosh, E. A., Paez-Espino, D., Jarett, J., Dunfield, P. F., Hedlund, B. P., Dekas, A. E., … Ivanova, N. N. (2016). Global metagenomic survey reveals a new bacterial candidate phylum in geothermal springs. *Nature Communications*, *7*, 10476.

Finn, R. D., Clements, J., & Eddy, S. R. (2011). HMMER web server: interactive sequence similarity searching. *Nucleic Acids Research*, *39*(suppl), W29–W37.

Finn, Robert D., Coggill, P., Eberhardt, R. Y., Eddy, S. R., Mistry, J., Mitchell, A. L., … Bateman, A. (2016). The Pfam protein families database: towards a more sustainable future. *Nucleic Acids Research*, *44*(D1), D279–D285.

Francino, M. P. (2012). The ecology of bacterial genes and the survival of the new. *International Journal of Evolutionary Biology*, *2012*, 394026.

Franzosa, E. A., McIver, L. J., Rahnavard, G., Thompson, L. R., Schirmer, M., Weingart, G., … Huttenhower, C. (2018). Species-level functional profiling of metagenomes and metatranscriptomes. *Nature Methods*, *15*(11), 962–968.

Habchi, J., Tompa, P., Longhi, S., & Uversky, V. N. (2014). Introducing protein intrinsic disorder. *Chemical Reviews*, *114*(13), 6561–6588.

Hanson, A. D., Pribat, A., Waller, J. C., & Crécy-Lagard, V. de. (2010). 'Unknown'proteins and 'orphan'enzymes: the missing half of the engineering parts list--and how to find it. *Biochemical Journal*, *425*(1), 1–11.

Hausser, J., & Strimmer, K. (2008). Entropy inference and the James-Stein estimator, with application to nonlinear gene association networks. Retrieved from http://arxiv.org/abs/0811.3579

Heffernan, B., Murphy, C. D., & Casey, E. (2009). Comparison of planktonic and biofilm cultures of Pseudomonas fluorescens DSM 8341 cells grown on fluoroacetate. *Applied and Environmental Microbiology*, *75*(9), 2899–2907.

Heinzinger, M., Elnaggar, A., Wang, Y., Dallago, C., Nechaev, D., Matthes, F., & Rost, B. (2019). Modeling aspects of the language of life through transfer-learning protein sequences. *BMC Bioinformatics*, *20*(1), 723.

Hingamp, P., Grimsley, N., Acinas, S. G., Clerissi, C., Subirana, L., Poulain, J., … Ogata, H. (2013). Exploring nucleo-cytoplasmic large DNA viruses in Tara Oceans microbial metagenomes. *The ISME Journal*, *7*(9), 1678–1695.

Höps, W., Jeffryes, M., & Bateman, A. (2018). Gene Unprediction with Spurio: A tool to identify spurious protein sequences. *F1000Research*, *7*, 261.

Huerta-Cepas, J., Forslund, K., Coelho, L. P., Szklarczyk, D., Jensen, L. J., von Mering, C., & Bork, P. (2017). Fast Genome-Wide Functional Annotation through Orthology Assignment by eggNOG-Mapper. *Molecular Biology and Evolution*, *34*(8), 2115–2122.

Huerta-Cepas, J., Szklarczyk, D., Heller, D., Hernández-Plaza, A., Forslund, S. K., Cook, H., …

Bork, P. (2019). eggNOG 5.0: a hierarchical, functionally and phylogenetically annotated orthology resource based on 5090 organisms and 2502 viruses. *Nucleic Acids Research*, *47*(D1), D309–D314.

Hug, L. A., Baker, B. J., Anantharaman, K., Brown, C. T., Probst, A. J., Castelle, C. J., … Banfield, J. F. (2016). A new view of the tree of life. *Nature Microbiology*, *1*, 16048.

Hyatt, D., Chen, G.-L., LoCascio, P. F., Land, M. L., Larimer, F. W., & Hauser, L. J. (2010). Prodigal: prokaryotic gene recognition and translation initiation site identification. *BMC Bioinformatics*, *11*(1), 119–119.

Ivanova, N. N., Schwientek, P., Tripp, H. J., Rinke, C., Pati, A., Huntemann, M., … Rubin, E. M. (2014). Stop codon reassignments in the wild. *Science*, *344*(6186), 909–913.

Jaroszewski, L., Li, Z., Krishna, S. S., Bakolitsa, C., Wooley, J., Deacon, M. A., … Godzik, A. (2009). Exploration of uncharted regions of the protein universe. *PLoS Biology*, *7*(9).

Jehl, P., Sievers, F., & Higgins, D. G. (2015). OD-seq: outlier detection in multiple sequence alignments. *BMC Bioinformatics*, *16*(1), 269–269.

Kopf, A., Bicak, M., Kottmann, R., Schnetzer, J., Kostadinov, I., Lehmann, K., … Glöckner, F. O. (2015). The ocean sampling day consortium. *GigaScience*, *4*, 27.

Köster, J. (2018). Reproducible data analysis with Snakemake. *F1000Research*, *7*. Retrieved from http://www.dodsc.tu-dortmund.de/cms/Medienpool/files/002_Kolloquium/09_Koester.pdf

La Cono, V., La Spada, G., Arcadi, E., Placenti, F., Smedile, F., Ruggeri, G., … Yakimov, M. M. (2013). Partaking of Archaea to biogeochemical cycling in oxygen-deficient zones of meromictic saline Lake Faro (Messina, Italy). *Environmental Microbiology*, *15*(6), 1717–1733.

Langfelder, P., Zhang, B., & Horvath, S. (2008). Defining clusters from a hierarchical cluster tree: the Dynamic Tree Cut package for R. *Bioinformatics* , *24*(5), 719–720.

Levins, R. (1966). THE STRATEGY OF MODEL BUILDING IN POPULATION BIOLOGY.

American Scientist, *54*(4), 421–431.

Li, H., & Durbin, R. (2010). Fast and accurate long-read alignment with Burrows–Wheeler transform. *Bioinformatics* , *26*(5), 589–595.

Li, W., & Godzik, A. (2006). Cd-hit: a fast program for clustering and comparing large sets of protein or nucleotide sequences. *Bioinformatics* , *22*(13), 1658–1659.

Liu, X. L. (2017). Deep Recurrent Neural Network for Protein Function Prediction from Sequence (p. 103994). doi:10.1101/103994

Lloyd-Price, J., Mahurkar, A., Rahnavard, G., Crabtree, J., Orvis, J., Hall, A. B., … Huttenhower, C. (2017). Strains, functions and dynamics in the expanded Human Microbiome Project. *Nature*, *550*(7674), 61–66.

Lobb, B., Kurtz, D. A., Moreno-Hagelsieb, G., & Doxey, A. C. (2015). Remote homology and the functions of metagenomic dark matter. *Frontiers in Genetics*, *6*(JUL), 1–12.

Ma, Y., Madupu, R., Karaoz, U., Nossa, C. W., Yang, L., Yooseph, S., … Pei, Z. (2014). Human papillomavirus community in healthy persons, defined by metagenomics analysis of human microbiome project shotgun sequencing data sets. *Journal of Virology*, *88*(9), 4786–4797.

Martiny, A. C., Treseder, K., & Pusch, G. (2013). Phylogenetic conservatism of functional traits in microorganisms. *The ISME Journal*, *7*(4), 830–838.

Matsen, F. A., Kodner, R. B., & Armbrust, E. V. (2010). pplacer: linear time maximum-likelihood and Bayesian phylogenetic placement of sequences onto a fixed reference tree. *BMC Bioinformatics*, *11*, 538.

Méheust, R., Burstein, D., Castelle, C. J., & Banfield, J. F. (2019). The distinction of CPR bacteria from other bacteria based on protein family content. *Nature Communications*, *10*(1), 4173.

Mendler, K., Chen, H., Parks, D. H., Lobb, B., Hug, L. A., & Doxey, A. C. (2019). AnnoTree: visualization and exploration of a functionally annotated microbial tree of life. *Nucleic*

Acids Research, *47*(9), 4442–4448.

Miklós, I., & Podani, J. (2004). RANDOMIZATION OF PRESENCE–ABSENCE MATRICES: COMMENTS AND NEW ALGORITHMS. *Ecology*, Vol. 85, pp. 86–92. doi:10.1890/03-0101

Mitchell, A. L., Almeida, A., Beracochea, M., Boland, M., Burgin, J., Cochrane, G., … Finn, R. D. (2020). MGnify: the microbiome analysis resource in 2020. *Nucleic Acids Research*, *48*(D1), D570–D578.

Muller, E. E. L. (2019). Determining Microbial Niche Breadth in the Environment for Better Ecosystem Fate Predictions. *MSystems*, *4*(3). doi:10.1128/mSystems.00080-19

Murat Eren, A., Esen, Ö. C., Quince, C., Vineis, J. H., Morrison, H. G., Sogin, M. L., & Delmont, T. O. (2015). Anvi'o: an advanced analysis and visualization platform for 'omics data. *PeerJ*, *3*, e1319.

NCBI Resource Coordinators. (2018). Database resources of the National Center for Biotechnology Information. *Nucleic Acids Research*, *46*(D1), D8–D13.

Needham, D. M., Yoshizawa, S., Hosaka, T., Poirier, C., Choi, C. J., Hehenberger, E., … Worden, A. Z. (2019). A distinct lineage of giant viruses brings a rhodopsin photosystem to unicellular marine predators. *Proceedings of the National Academy of Sciences of the United States of America*, *116*(41), 20574–20583.

Olson, D. K., Yoshizawa, S., Boeuf, D., Iwasaki, W., & DeLong, E. F. (2018). Proteorhodopsin variability and distribution in the North Pacific Subtropical Gyre. *The ISME Journal*, *12*(4), 1047–1060.

Pachiadaki, M. G., Brown, J. M., Brown, J., Bezuidt, O., Berube, P. M., Biller, S. J., … Stepanauskas, R. (2019). Charting the Complexity of the Marine Microbiome through Single-Cell Genomics. *Cell*, *179*(7), 1623-1635.e11.

Parks, D. H., Chuvochina, M., Waite, D. W., Rinke, C., Skarshewski, A., Chaumeil, P.-A., & Hugenholtz, P. (2018). A standardized bacterial taxonomy based on genome phylogeny

substantially revises the tree of life. *Nature Biotechnology*, *36*(10), 996–1004.

Pasolli, E., Asnicar, F., Manara, S., Zolfo, M., Karcher, N., Armanini, F., … Segata, N. (2019). Extensive Unexplored Human Microbiome Diversity Revealed by Over 150,000 Genomes from Metagenomes Spanning Age, Geography, and Lifestyle. *Cell*, *176*(3), 649-662.e20.

Perdigão, N., Rosa, A. C., & O'Donoghue, S. I. (2017). The Dark Proteome Database. *BioData Mining*, *10*(1), 1–11.

Price, M. N., Wetmore, K. M., Waters, R. J., Callaghan, M., Ray, J., Liu, H., … Deutschbauer, A. M. (2018). Mutant phenotypes for thousands of bacterial genes of unknown function. *Nature*, *557*(7706), 503–509.

Quince, C., Walker, A. W., Simpson, J. T., Loman, N. J., & Segata, N. (2017). Shotgun metagenomics, from sampling to analysis. *Nature Biotechnology*, *35*(9), 833–844.

Quinlan, A. R., & Hall, I. M. (2010). BEDTools: a flexible suite of utilities for comparing genomic features. *Bioinformatics* , *26*(6), 841–842.

Remmert, M., Biegert, A., Hauser, A., & Söding, J. (2012). HHblits: Lightning-fast iterative protein sequence searching by HMM-HMM alignment. *Nature Methods*, *9*(2), 173–175.

Rinke, C., Schwientek, P., Sczyrba, A., Ivanova, N. N., Anderson, I. J., Cheng, J.-F., … Woyke, T. (2013). Insights into the phylogeny and coding potential of microbial dark matter. *Nature*, *499*(7459), 431–437.

Rost, B. (1999). Twilight zone of protein sequence alignments. *Protein Engineering, Design & Selection: PEDS*, *12*(2), 85–94.

Roumpeka, D. D., Wallace, R. J., Escalettes, F., Fotheringham, I., & Watson, M. (2017). A Review of Bioinformatics Tools for Bio-Prospecting from Metagenomic Sequence Data. *Frontiers in Genetics*, *8*, 23.

Rusch, D. B., Halpern, A. L., Sutton, G., Heidelberg, K. B., Williamson, S., Yooseph, S., … Venter, J. C. (2007). The Sorcerer II Global Ocean Sampling Expedition: Northwest

Atlantic through Eastern Tropical Pacific. *PLoS Biology*, *5*(3), 1–34.

Salazar, G., Cornejo-Castillo, F. M., Borrull, E., Díez-Vives, C., Lara, E., Vaqué, D., … Acinas, S. G. (2015). Particle-association lifestyle is a phylogenetically conserved trait in bathypelagic prokaryotes. *Molecular Ecology*, *24*(22), 5692–5706.

Salazar, G., Paoli, L., Alberti, A., Huerta-Cepas, J., Ruscheweyh, H.-J., Cuenca, M., … Sunagawa, S. (2019). Gene Expression Changes and Community Turnover Differentially Shape the Global Ocean Metatranscriptome. *Cell*, *179*(5), 1068-1083.e21.

Sanger, F., Nicklen, S., & Coulson, A. R. (1977). DNA sequencing with chain-terminating inhibitors. *Proceedings of the National Academy of Sciences of the United States of America*, *74*(12), 5463–5467.

Sberro, H., Fremin, B. J., Zlitni, S., Edfors, F., Greenfield, N., Snyder, M. P., … Bhatt, A. S. (2019). Large-Scale Analyses of Human Microbiomes Reveal Thousands of Small, Novel Genes. *Cell*, *178*(5), 1245-1259.e14.

Scales, B. S., Dickson, R. P., LiPuma, J. J., & Huffnagle, G. B. (2014). Microbiology, genomics, and clinical significance of the Pseudomonas fluorescens species complex, an unappreciated colonizer of humans. *Clinical Microbiology Reviews*, *27*(4), 927–948.

Skewes-Cox, P., Sharpton, T. J., Pollard, K. S., & DeRisi, J. L. (2014). Profile hidden Markov models for the detection of viruses within metagenomic sequence data. *PloS One*, *9*(8), e105067.

Spang, A., Saw, J. H., Jørgensen, S. L., Zaremba-Niedzwiedzka, K., Martijn, J., Lind, A. E., … Ettema, T. J. G. (2015). Complex archaea that bridge the gap between prokaryotes and eukaryotes. *Nature*, *521*(7551), 173–179.

Stamatakis, A. (2014). RAxML version 8: a tool for phylogenetic analysis and post-analysis of large phylogenies. *Bioinformatics* , *30*(9), 1312–1313.

Steinegger, M., Meier, M., Mirdita, M., Vöhringer, H., Haunsberger, S. J., & Söding, J. (2019). HH-suite3 for fast remote homology detection and deep protein annotation. *BMC*

Bioinformatics, *20*(1), 473.

Steinegger, M., Mirdita, M., & Söding, J. (2019). Protein-level assembly increases protein sequence recovery from metagenomic samples manyfold. *Nature Methods*, *16*(7), 603–606.

Steinegger, M., & Salzberg, S. L. (2020). Terminating contamination: large-scale search identifies more than 2,000,000 contaminated entries in GenBank. *Genome Biology*, *21*(1), 115.

Steinegger, M., & Soding, J. (2017). MMseqs2 enables sensitive protein sequence searching for the analysis of massive data sets. *Nature Biotechnology*, *advance on*. doi:10.1038/nbt.3988

Steinegger, M., & Söding, J. (2018). Clustering huge protein sequence sets in linear time. *Nature Communications*, *9*(1), 2542.

Sunagawa, S., Coelho, L. P., Chaffron, S., Kultima, J. R., Labadie, K., Salazar, G., … Bork, P. (2015). Ocean plankton. Structure and function of the global ocean microbiome. *Science*, *348*(6237), 1261359.

The UniProt Consortium. (2017). UniProt: the universal protein knowledgebase. *Nucleic Acids Research*, *45*(D1), D158–D169.

Thomas, A. M., & Segata, N. (2019). Multiple levels of the unknown in microbiome research. *BMC Biology*, *17*(1), 48.

Titus Brown, C., Moritz, D., O'Brien, M. P., Reidl, F., Reiter, T., & Sullivan, B. D. (2018). Exploring neighborhoods in large metagenome assembly graphs reveals hidden sequence diversity (p. 462788). doi:10.1101/462788

UniProt Consortium, T. (2018). UniProt: the universal protein knowledgebase. *Nucleic Acids Research*, *46*(5), 2699.

van Dongen, S., & Abreu-Goodger, C. (2012). Using MCL to Extract Clusters from Networks. In J. van Helden, A. Toussaint, & D. Thieffry (Eds.), *Bacterial Molecular Networks: Methods*

and Protocols (pp. 281–295). New York, NY: Springer New York.

Vanhoutreve, R., Kress, A., Legrand, B., Gass, H., Poch, O., & Thompson, J. D. (2016). LEON-BIS: multiple alignment evaluation of sequence neighbours using a Bayesian inference system. *BMC Bioinformatics*, *17*(1), 271–271.

Vorobev, A., Dupouy, M., Carradec, Q., Delmont, T., Annamale, A., Wincker, P., & Pelletier, E. (2020). Transcriptome reconstruction and functional analysis of eukaryotic marine plankton communities via high-throughput metagenomics and metatranscriptomics. *Genome Research*. doi:10.1101/gr.253070.119

Wyman, S. K., Avila-Herrera, A., Nayfach, S., & Pollard, K. S. (2018). A most wanted list of conserved microbial protein families with no known domains. *PloS One*, *13*(10), e0205749.

Yooseph, S., Li, W., & Sutton, G. (2008). Gene identification and protein classification in microbial metagenomic sequence data via incremental clustering. *BMC Bioinformatics*, *9*, 1–13.

Yooseph, S., Sutton, G., Rusch, B. D., Halpern, L. A., Williamson, J. S., Remington, K., … Venter, C. J. (2007). The Sorcerer II global ocean sampling expedition: Expanding the universe of protein families. *PLoS Biology*, *5*(3), 0432–0466.

Žure, M., Fernandez-Guerra, A., Munn, C. B., & Harder, J. (2017). Geographic distribution at subspecies resolution level: closely related Rhodopirellula species in European coastal sediments. *The ISME Journal*, *11*(2), 478–489.